Engineered wood products for circular construction: a multi-factor evaluation of lamination methods

Check for updates

Dan Bergsagel[1,2], Felix Heisel[1] ✉, Jasper Owen[1] & Maxwell Rodencal[1]

Engineered wood products (EWP) constitute a diverse range of structural element types attractive for the current construction industry. However, the use of permanent adhesive resins limits their ability to perform within a circular economy, and the glue-laminating process requires fossil-fuel-based adhesives that release potentially harmful gases. This paper presents a multi-factor evaluation of alternative lamination methods featuring an enhanced longitudinal shear transfer mechanism to produce beam elements with comparable structural performance while improving circular and environmental performance. The research focuses on EWP beam elements following three sequential studies: (1) an evaluation of interlocking surface patterns to improve non-adhesive lamination in two stages, interlocking pattern shapes (17 samples) and interlocking depths (24 samples); (2) an evaluation of structural performance of different lamination methods in bending (glue (GL), metal nails (MN), wood nails (WN), plastic straps (PS)) for a 4.5 ft two-layer beam formed of 2 × 4 lumber feedstock (using a 1/16in deep square grooved pattern and flat interface for reference (five samples each)), whereby the grooved interlocking samples with mechanical fasteners performed considerably well in both modulus of rupture (MOR) and modulus of elasticity (MOE) compared to the reference flat adhesive lamination method, 31% and 19% lower, respectively; and (3) a comparison of qualitative and quantitative parameters on structure, economy, environment and circularity. Together, the study identified a grooved shear interface with wood nail fasteners as a preferred lamination method for EWPs in circular construction (GrooveLam). These results are considered appropriate for the future development of larger dimension and longer length multi-lamination structural bending elements.

Driven by both environmental, as well as design and engineering considerations, the importance of engineered wood products (EWP) in the architecture, engineering, and construction (AEC) industries continues to grow. In times of increasing demand and depleting sources of sustainably harvested timber, EWPs allow the use of shorter, smaller-dimension wood elements—such as dimensional lumber—to be combined to form longer, large-dimension structural elements such as glue-laminated timber (glulam) and cross-laminated timber (CLT)[1]. The use of EWPs that can span longer distances than feasible with the available solid wood cross-sections and lengths[2] has supported industry trends for wood buildings with wider column grid spacing and more flexible programming. Recent trends in demonstrating the sustainability of a building through embodied carbon calculations have further promoted the growth of EWPs as a sustainable structural material in comparison to steel and concrete structural frame systems[3]. EWPs have proven a versatile material for designers, enabling the execution of traditional joinery or complex digital fabrication[4]. EWPs have also proven a competitive material in ever-more challenging structural systems, ranging from multi-story buildings[5] to long-span roofs[6]. Still, the volume of EWPs currently contributes less than 1% of the total wood products industry in the US[7].

Most EWPs are manufactured by finger jointing shorter pieces of lumber end-to-end to make longer lengths and laminating these longer lengths face-to-face using adhesives to make wider and deeper elements[8]. The mechanical properties of the primary input material are versatile: wood has a high specific strength (strength-to-density ratio) and specific modulus (stiffness-to-density ratio), which makes it suitable for designs with minimum weight[9], is easy to cut and work with in the shop and on-site, and is a renewable resource. The inherent variability in wood properties is partially

[1]Circular Construction Lab, Department of Architecture, Cornell University, Ithaca, NY, USA. [2]Schlaich Bergermann Partner, New York, NY, USA.
✉e-mail: felix.heisel@cornell.edu

overcome through the lamination process, where the impact of defects is distributed to produce higher-strength EWPs from lower-strength feedstock.

However, status quo EWPs have identified issues when considering circularity and health. Circular economy principles aim to reduce the environmental impact of the construction industry[10]. A key tenet of circular construction is an approach that favors extending the lifespan of existing structural elements at the end of their current use through reuse, repair, or high-level remanufacturing, as opposed to landfill, energy recovery, recycling, or downcycling[11,12]. Current methodologies exist for assessing the design values of glulam within existing structures[13], and studies have outlined assessment methods for determining the reuse potential of glulam elements once removed from a structure[14]. However, current regulations are envisaged only for the structural use of newly-manufactured and marked glulam members as opposed to the direct structural reuse of EWPs, for example, the International Building Code (IBC) in the US[15]. The standards that control the manufacture of EWP products also restrict the wood feedstock to strength graded wood[16,17], which currently excludes the use of reclaimed wood.

Status-quo commercial EWPs are made exclusively with virgin wood feedstock as opposed to reclaimed wood, partly due to the existing barriers to structural reuse[18] but also due to uncertainties related to the use of adhesives and machinery with wood that has aged and may have fewer even surfaces[19]. This precludes the use of existing reclaimed wood resources in lieu of newly felled virgin wood resources, while the environmental benefits[20] and supply-chain benefits of reusing reclaimed wood elements are beneficial for a global forestry resource in increasingly high demand[21]. The process of laminating wood with adhesives is irreversible. EWPs can only be returned to their individual initial feedstock elements through sawing or be reconfigured into different element dimensions through sawing and re-gluing. Sawing and regluing EWPs can limit their future use for structural purposes as post-processing can contravene EWP manufacturing regulations[16] and the repetition of these EWP processes accumulates the associated costs, time, and environmental impacts[22].

There are also disadvantages to the use of EWPs associated with their manufacturing process. Recent reviews have summarized works that indicate adhesive resins commonly used to laminate wood are toxic to humans[23]. These resins are also controlled in some sustainability ranking systems, such as being included on the Living Building Challenge Red List[24], due to concerns related to formaldehyde and volatile organic compounds (VOC). The environmental impact of the production of glulam is related to the energy used in manufacture, with over 50% associated with drying wood and producing resins[25]. This energy use could be avoided by using wood, which does not require drying, and by seeking alternatives to resin lamination.

For projects that strive to be healthy, sustainable, and embody circular economy principles, there may be advantages to using circular and reversible laminating methods that: minimize toxicity and environmental impact; allow for diverse reclaimed dry wood elements to be used as feedstock; and allow for potential future reuse of the feedstock and/or product.

EWPs can be divided into four element types: (a) one-way-spanning panel products, where the lamination surface is in the same plane as the applied load; (b) two-way spanning shear panel products, where the lamination surface is perpendicular to the plane in which the load is applied and the lamination direction varies between layers; (c) beam products, where the lamination surface is perpendicular to the plane in which the load is applied and all laminations are in the same direction; and (d) column products, where the lamination surface is perpendicular to the primary buckling direction Fig. 1). To address the above limitations, EWPs can be made with alternative lamination methods to conventional adhesives that transfer shear between adjacent dimensional lumber elements. The methods reviewed here are selected based on their avoidance of adhesives, and their potential to perform within a circular economy.

One-way panel products use lamination to connect layers perpendicular to the load direction to distribute load to adjacent structural elements. The thickness of the panel is defined by one individual dimensional lumber element; therefore, the primary bending strength and out-of-plane stiffness of the panel is defined by the size of the dimensional lumber chosen. The selection of the dimensional lumber is therefore critical to the structural performance as opposed to the effectiveness of the lamination. There exist several EWP panels made without adhesives, such as conventional stress-laminated timber (SLT), dowel-laminated timber (DLT), and nail-laminated timber (NLT), in addition to some less-common variations.

SLT panels are made from individual dimensional lumber elements positioned face-to-face and stressed against one another using high-strength steel threaded rods that pass through a complete panel of elements. The clamping pre-stress applied through tightening the rod generates friction, which allows the applied load to be transmitted between adjacent dimensional lumber elements[26]. SLT is reversible—the steel threaded rods can be destressed and removed—leaving individual dimensional lumber elements with holes drilled in the center of their face at a regular spacing. The size and spacing of these holes can be a barrier to future reuse.

DLT panels are made from individual dimensional lumber elements positioned face-to-face and connected with friction-fit hardwood dowels that pass through a complete panel of elements[8]. The dowels transfer the shear between elements. As the dowels are made of wood, the DLT panel can be reprocessed with conventional woodworking equipment without the fear of metal fasteners damaging the machines. However, as the dowels are designed as a friction fit, they are hard to remove. As with SLT, once the hardwood dowels are removed, the holes in the individual dimensional lumber elements persist, reducing the reuse potential of the elements.

NLT panels are made from individual dimensional lumber elements positioned face-to-face and connected with common metal nails. The nails connect each piece of lumber to one or two adjacent pieces only and do not pass through the whole panel. The complete panel is interconnected by a staggered nailing pattern[27]. The metal fasteners prevent the NLT panel from being reprocessed without the risk of damaging conventional woodworking equipment. The nails can be removed from the panel to return the constituent dimensional lumber to individual elements; however, the process of removing nails is labor-intensive and can cause damage to the lumber. Once the nails are removed, small holes will persist in the individual lumber elements; however, due to their small size, their impact on future structural performance is reduced compared to the larger holes from SLT or DLT manufacturing. NLT panels are easy to fabricate as fasteners can be installed with a pneumatic air gun. SLT and DLT are harder to fabricate as they require additional equipment and a higher level of skill to predrill the holes to receive the threaded rods and dowels.

Alternative non-adhesive methods for fabricating EWP panels involve variations on these common products, such as the use of compressed wood dowels as opposed to hardwood[28] and diagonal dowel arrangements in DLT[29,30], and the use of screws as opposed to nails in NLT[31].

This category comprises beam, column, and two-way panel products that use lamination to connect elements layered in the direction of the load. The depth of the beam or the thickness of the panel is defined by a combination of individual dimensional lumber elements. Therefore, the primary bending strength and stiffness of the element are defined by both the number of layers of dimensional lumber chosen and the effectiveness of the lamination method in transferring longitudinal shear between the individual elements. For beam, column, and two-way panel products, in addition to evaluating their potential performance within a circular economy, we must also review the structural performance of the lamination in strength and stiffness. Beam, column, and two-way panel products are fabricated using similar methods to one-way panels, employing stress, wood dowels, and metal fasteners to transfer shear between elements.

Built-up columns are mechanically laminated with either common metal nails or metal bolts. Their use enables dimensional lumber to form similar cross-sections to large-dimension timber posts, and they are considered part of the conventionally available range of structural design solutions. The buckling stability of a built-up columns fabricated according to the National Design Specification is governed by equations relating to whether the buckling length is calculated in the laminated direction—which
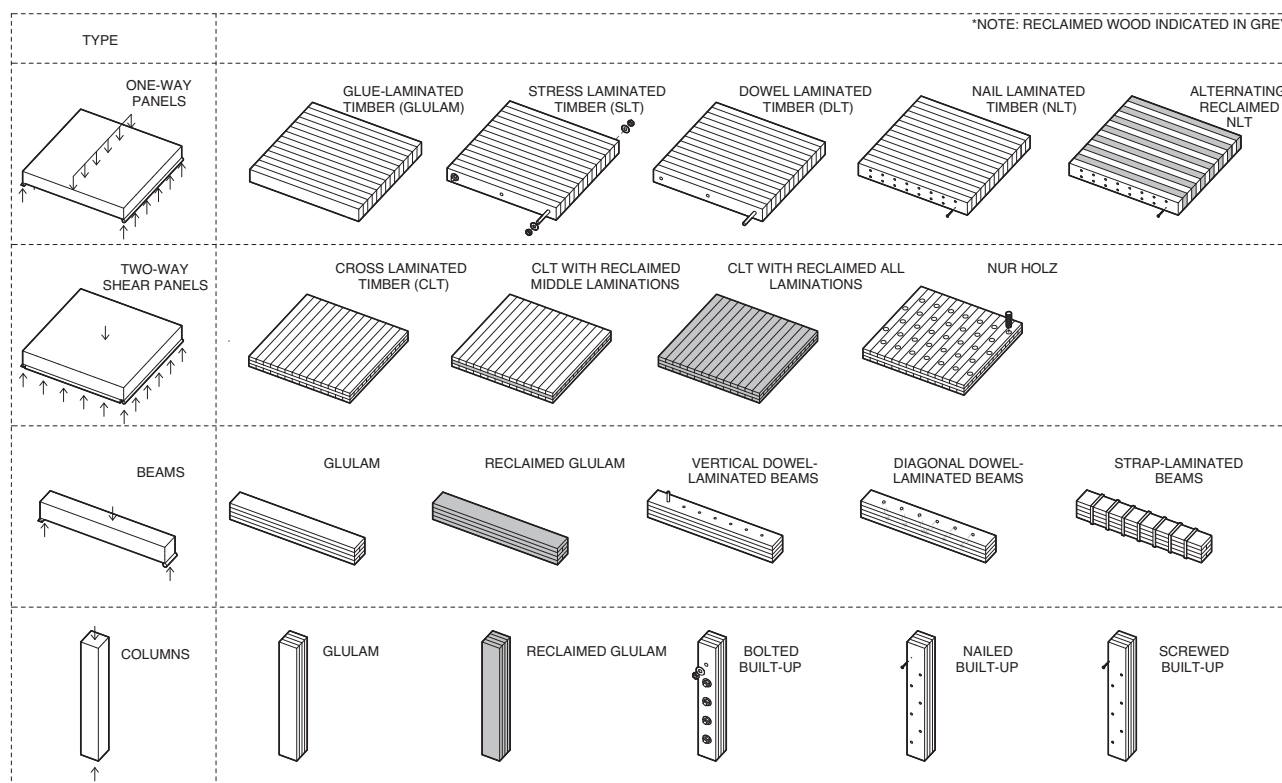
Fig. 1 | Engineered wood product typology categories. The left column indicates structural element types based on geometry, loads and support conditions. The right column indicates the range of engineered wood product categories available to manufacture each element type.

employs a reduction factor associated with nailed ($K_f = 0.6$) or bolted fasteners ($K_f = 0.75$)—or the unlaminated direction—where no reduction factor is applied ($K_f = 1.0$)[32]. The potential to reuse the dimensional lumber feedstock of built-up columns is similar to that for SLT for bolted columns, and NLT for nailed columns.

Beams laminated without adhesives are uncommon in practice, with most examples confined to academic research. A recent review[33] described a range of beams fabricated following different variations on DLT principles —such as single or multiple rows of dowels, angled dowels, or dowels installed with a band using high-speed rotational welding. The DLT beams generally exhibit lower stiffness and lower failure loads than equivalent glued-laminated beams, but they recorded a more ductile response compared to glulam[33]. A study that compared beams mechanically laminated with inclined wood screws against a reference glulam beam of the same dimensions showed similar strength performance but a reduced stiffness performance for the laminated beams[34]. The potential to reuse the dimensional lumber feedstock of DLT beams is similar to that for DLT, with a denser spacing of holes in the dimensional lumber due to the higher shear transfer requirements of a beam as opposed to a one-way panel.

Two-way panels laminated without adhesives have been proposed in research[28], but also utilized in construction. The Nur Holz system, using threaded dowel laminated multi-layer panels, has received European Technical Approval and has been primarily used as shear walls and diaphragm slabs[35].

SLT beams have an advantage over SLT panels in that the stressing elements can pass around the outside of the beam instead of through it. This means that SLT beams do not require holes to be drilled through the dimensional lumber feedstock, but instead, straps can be tightened around the outside of the beam section. The circular construction advantages of this principle were used for the construction of the People's Pavilion in Eindhoven in 2017, where the aim of the project was to return all the construction materials to their original sources after the disassembly of the pavilion. Steel straps were tightened around the beam to clamp the dimensional lumber

laminations together to allow for shear transfer between the laminations through friction[36]. No holes were drilled through the dimensional lumber, however, the force applied by the steel straps led to some damage to the wood at the corners of the elements. There is no publicly available structural performance data related to the stiffness or strength of the SLT beams from this project. Other potential negative impacts of external strapping, such as complications when coordinating connections between the SLT steel strap beams to other elements within the structure, are also not discussed.

EWPs can also be manufactured using bio-based non-synthetic adhesives that are not fossil-fuel derived and do not off-gas toxic chemicals such as formaldehyde. A range of bio-adhesives is available for use with wood, and can be categorized into five groups: using lignin, proteins, tannins, carbohydrates, and polyhydroxyalkanoates[37]. Many of these adhesives have been historically used to laminate timber and have demonstrated long-term performance in interior conditions[38], before their replacement with synthetic resins in the 1970s[39].

When compared to conventional wood adhesives for lamination, such as phenol-formaldehyde or polyurethane, these bio-based adhesives can minimize the environmental and human health impacts of laminating wood with conventional adhesives[40]. However, entirely biological adhesives demonstrate low strength and durability[37]. Instead, recent research in the application of lower environmental impact adhesives for laminating wood has focused on reducing the dependence on petrochemical sources but not eliminating them, either by substituting phenol in a phenol-formaldehyde adhesive with lignin[40], or substituting natural proteins for polyols in polyurethane adhesive systems[41]. While these partially biological adhesives have demonstrated good structural performance and reduced environmental and health impacts, they do not eliminate the use of petrochemicals or the off-gassing of formaldehyde. The use of bio-based adhesives does not improve the circularity of EWPs, as the laminations are still irreversibly bonded.

Reclaimed wood is sourced through deconstruction: the act of safely, carefully, and systematically dismantling a building or structure with the goal to maximize the recovery of valuable materials and architectural

　　　　　　　　　　　　　　　　　　　　　　　　　　　　　　　　　　　Article

components for reuse or recycling[11]. Several recent case studies in the US context have demonstrated the technical and economic feasibility of deconstruction, as well as the social and environmental benefits of deconstruction and material reuse over demolition and landfilling[42,43] demonstrates the potential of deconstruction at scale, estimating 3 billion USD in economic impact and 12,600 new jobs assuming 75% of residential demolitions in New York State would be executed as deconstruction projects. This change in building removal from demolition to deconstruction could also make available 421,000 tons of construction materials for direct reuse, including large quantities of high-quality lumber (grade 2 or higher).

The use of reclaimed wood in EWPs has been explored using different laminating techniques. The majority of work has focused on laminating reclaimed wood using conventional adhesives, with research exploring alternative methods of fabricating and evaluating CLT[44–46] and glulam[19]. Some of these studies also explored using combinations of virgin and reclaimed wood for laminations depending on fabrication and load scenarios[44,47]. Research at UCL is currently working towards the commercialization of CLT made from reclaimed wood, named cross-laminated secondary timber (CLST)[48,49]. Many of these studies have demonstrated the viability of using reclaimed wood, however in all situations the reclaimed wood undergoes processing prior to lamination that regularizes and reduces its cross-section, either through planing the dimensional lumber to meet the required lamination thicknesses for existing fabrication standards, or planing to produce an improved surface for the laminating adhesive. While the use of reclaimed material reduced the need for virgin resources, glulam and CLT that use reclaimed wood with conventional adhesives present no ongoing advantages over virgin wood adhesive-laminated EWPs in terms of end-of-use circularity.

Reclaimed wood was successfully incorporated into the NLT panel flooring of the Kendeda building[50], however, in this project, the reclaimed dimensional lumber was alternated in the panel with virgin dimensional lumber, with the structural calculations considering only the contributions of the virgin dimensional lumber. Reclaimed wood was also incorporated within mechanically built-up column sections of the Circulating Matters project. However, the built-up section in this case was considered only for geometric compliance and connections between elements, and not to enhance the overall strength and stiffness of the wood used in the central lamination of the column[18]. Recent research at the University of Stuttgart has explored the use of reclaimed wood as part of a beam laminated without adhesives, where a clay plaster-mortar mixture is used in combination with twisted jute fibers to provide some clamping laminating force to uneven and non-rectangular, non-prismatic reclaimed wood sections[51]. Structural comparisons were not made for these beams against equivalent EWPs using adhesives. While the reclaimed wood elements could technically be extracted from the beam through the removal of the fibers and the cleaning of the applied clay plaster-mortar, the practicalities of removing the clay and the specific feedstock of wood elements with irregular dimensions reduce the value of these elements for alternate uses.

The implementation of novel structural systems that do not laminate elements directly but select a system to explicitly allow for the heterogeneous nature of reclaimed wood reuse—such as the reinterpreted Hilding Brosenius beam—is another interesting example of developments in using reclaimed wood as feedstock for EWPs[52].

Results
EWP for circular construction
This paper presents a multi-factor evaluation of circular and reversible lamination methods in EWPs. The study focuses on lamination methods for beam elements: beams are an efficient use of wood material as they benefit from wood's high specific modulus for stiffness-controlled minimum-weight design. EWP beams gain their strength and stiffness from the lamination method, and as one-way spanning elements, they are suitable for developing a clear experimental testing methodology with conventional laboratory equipment.

The study considers lamination methods for EWP beam elements that vary both the fastener type used to laminate the dimensional lumber and whether the interface surface of the dimensional lumber elements is flat or incorporates interlocking elements. The lamination of elements incorporates two mechanisms to prevent sliding between the dimensional lumber, and to prevent separation. Varying the fastener type with a flat planed interface surface studies the relative performance of different fasteners in preventing both sliding and separation. Varying the fastener type in combination with an interlocking surface allows the study of the importance of the fastener, primarily to avoid separation. In total, eight different lamination methods were evaluated for grooved (GR) and flat (FL) interface surface types—using glue (GL), metal nails (MN), wood nails (WN), and plastic straps (PS) (Fig. 2).

Each lamination method is evaluated against multiple criteria using quantitative experimental data and qualitative assessments. These criteria are also grouped into broader evaluation categories, such as: structure, economy, environment, or circularity (Table 1).

This paper contains three sequential studies that together enable the multi-factor evaluation of lamination methods for EWPs within a circular construction strategy. The first study selects a suitable lamination interlocking surface pattern hypothesized to improve non-adhesive lamination. This selection was completed in two stages, first, evaluating different interlocking pattern profiles, and then evaluating their interlocking depth. These interlocking studies were completed on small 2in × 2.75in × 1–7/8in shear test samples. The second study evaluates the structural performance of lamination methods for a beam in bending, incorporating the shear interlocking surface selected in the first study. These lamination studies were completed on 2.75in × 3.5in × 52in two-lamination fabricated EWP beams. The second study focuses on the lamination method between layers when fabricating EWPs—therefore all EWPs are fabricated as the width of one-dimensional lumber elements and without the presence of finger joints. The cross-section aspect ratio and dimensions of the beam element samples tested in this paper are used only to explore the structural impact of the different interlocking lamination methods and are not proposed as a prototype for structural elements; these samples are a study in the lamination method that could make up larger-scale multi-layer beams. The third study evaluates the economic, environmental, and circular performance of these lamination methods based on a comparison between the different lamination method test samples.

### Interlocking profile and pattern exploration
The results of the series 1 exploratory structural tests were paired against the manufacturing parameters to select the highest performing interlocking profile and pattern. A high-performing interlocking surface treatment was defined as one that balances structural performance parameters—a high maximum load capacity, high stiffness, and a low load perpendicular to the surface—against the economic burden of manufacturing the surface—a low loss of milled material and a fast fabrication time. A high maximum load capacity and high interlocking stiffness are the primary structural goals of an interface that prevents sliding between two wood elements.

In conjunction with high capacity and stiffness, it is desirable to have a low load perpendicular to the interface surface. The project aimed to test a range of fastener types, such as adhesives, nails, dowel fasteners, and straps. Minimizing the required capacity of the fastening mechanism between two wood elements allows for greater flexibility in the types of dowel fasteners that could be used with low withdrawal capacities. If external straps are used, minimizing the load perpendicular to the interface surface reduces the stress concentrations and potential crushing where the straps load the wood perpendicular to the grain, limiting damage to the wood.

The maximum load capacity and interface surface displacement in the exploratory series 1 tests are shown in Fig. 3. The interlocking surface treatment results reveal a large variation in the maximum load capacity, from approximately 1300–3800 N. Figure 3 also reveals a large variation in displacement at maximum load, from less than 1.5 mm to nearly 5 mm. The interlocking surfaces profiles are broadly split into two categories: square

Fig. 2 | Visual summary of lamination methods. In this matrix, columns indicate the interface type while rows indicate the fastener type.
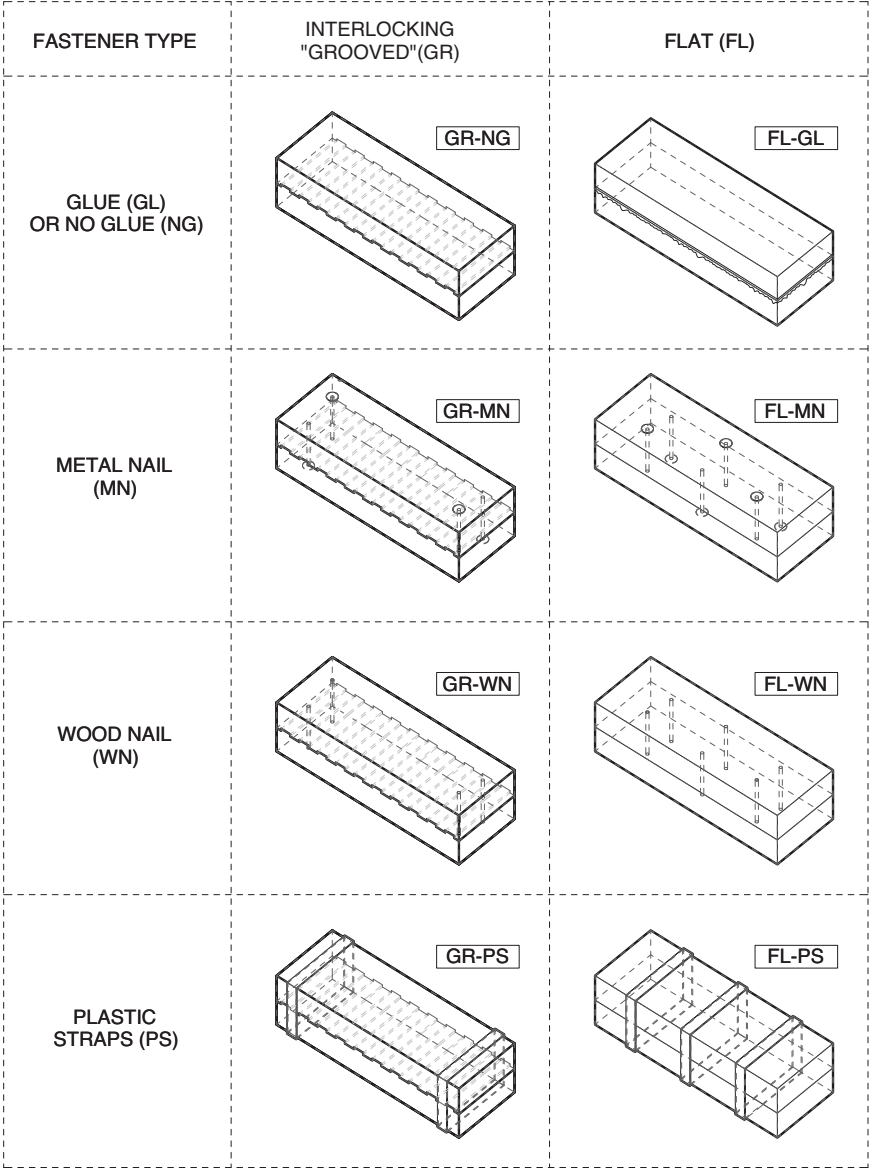
Table 1 | Quantitative and qualitative evaluation criteria

| Category	Criteria	
	Quantitative	Qualitative
Structure	Strength	
	Stiffness	Failure mechanism
Economy	Waste	
	Production time	
	Cost	
Environment	LCA	Health
Circularity		Processability
		End-of-use scenarios

(SQ) and triangular (TR) wave patterns that exhibited approximately linear stiffness with smaller displacement and an abrupt total failure (Fig. 3b); and stepped (STEP), truncated triangle (TT), and pyramidal (PYRA) wave patterns that typically exhibited larger displacement and a non-linear reduction in stiffness as the maximum capacity of the interlocking surface was approached, followed by a progressive reduction in strength capacity before eventual failure (Fig. 3a). All interfaces failed through shear failure of the interlocking teeth, although the location of the shear failure could be distributed between the two sides of the surface. The difference in failure mode between the different profiles is related to the bearing surface and angle of the interlocking components.

The abrupt failure group had a higher maximum load capacity of 1868N or above, typically exhibited stiffer behavior, and had an approximately linear load-displacement curve when being initially loaded. The progressive reduction in capacity group had a lower maximum load capacity of 2506 N or below, typically exhibited less stiff behavior, and had a change in initial stiffness visible in the load-displacement curve, transition from a low stiffness to a higher stiffness after an initial displacement of 0.5–1.5 mm.

In a laminated beam, the strength and stiffness of the lamination material itself are expected to govern, with the lamination method/interlocking interface designed to have a higher strength and stiffness than the material it connects. In this context, abrupt failure is not a disadvantage, but here it correlates with a stiffer and higher capacity interlocking interface surface.

The interlocking surfaces with wider patterns—such as the triangular wide (TR-W) and truncated triangular (TT-W)—exhibited less stiff behavior and increasing load perpendicular to the surface as displacement
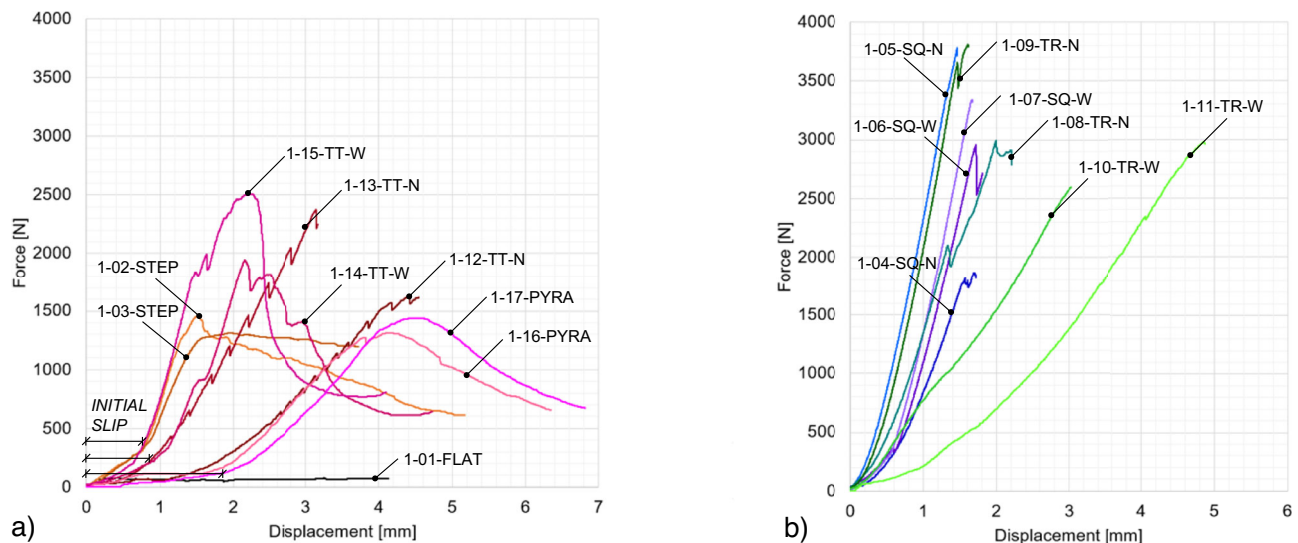
Fig. 3 | Series 1 interlocking surface exploratory tests—load, displacement, and load perpendicular to the surface. a Non-linear larger displacement failure and **b** approximately linear smaller displacement failure.
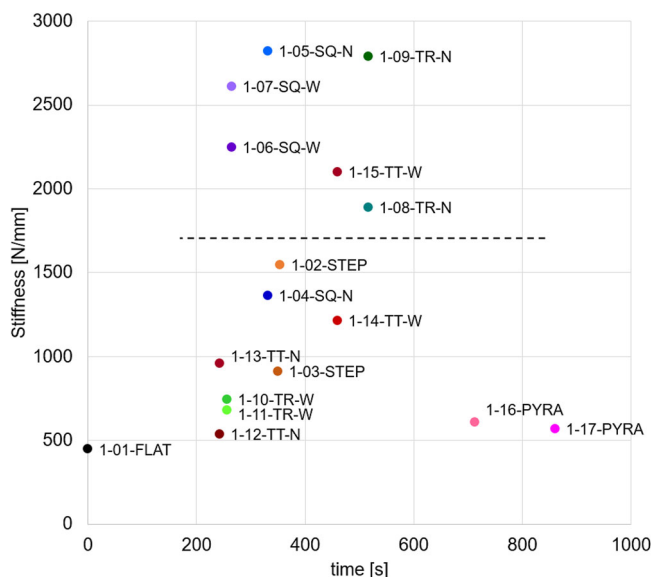
Fig. 4 | Series 1 interlocking surface exploratory tests - stiffness vs milling time. The dashed horizontal line indicates boundary between methods continued for further study and methods discontinued.

increased. This can be attributed to slipping between the interlocking interfaces and accumulative wedge action as the angled interlocking teeth of the interface surface push the two wood elements apart as they slide past one another.

The load perpendicular to the surface for each interlocking surface treatment was recorded in parallel to the load-displacement in the parallel direction of the interface. The abrupt failure group in Fig. 3b showed negligible perpendicular load for all but one test sample. Some samples in the group with a progressive reduction in capacity (Fig. 3a) recorded an increasing perpendicular load as the maximum capacity reduced, as caused by the wedge action of the angled teeth.

By selecting from the series 1 interlocking surfaces only the patterns with the best structural performance—patterns that exhibited low load perpendicular to the surface, high stiffness and high maximum load capacity from the exploratory test series—a short list of four profile types emerges, including: square narrow and wide (SQ-N and SQ-W), triangular narrow

(TR-N), and truncated triangular narrow (TT-N). These three profiles were selected for further consideration in the series 2 depth-selection tests.

The series 1 structural performance parameters can also be assessed in combination with manufacturing performance parameters. The milling volume—the total volume of wood removed to form the interlocking interface surface—was largely constant across the different profiles, with only a small variation in the stepped (STEP) and pyramidal (PYRA) types. Consequently, the milling volume does not appear to be a decisive parameter for selecting performance. The milling time—the total routing time needed to form each interlocking interface—exhibited more variation depending on the complexity of the pattern. Figure 4 plots the stiffness value for each interlocking interface surface against milling time. The stiffness was defined as the gradient of the load-displacement curve between the 20% and 50% of the maximum load capacity of each interlocking interface surface. The milling time is as noted in the methodology section. Similar relationships were also noted between maximum capacity and milling time, and milled volume.

The interlocking surfaces at the top of Fig. 4 (above the dashed line) have good structural behavior. The interlocking interface surfaces closest to the top left corner of the chart show both good structural and manufacturing performance. These are the square wave profiles (SQ-N, SQ-W), which exhibited high stiffness, and low milling time.

## Interlocking profile and pattern depth-selection

The results of the series 2 depth-selection structural tests were paired against the manufacturing parameters to select the highest performing interlocking profile and depth. The same selection criteria were used as for the series 1 tests: a high performing interlocking interface surface balances structural performance parameters—a high maximum load capacity, high stiffness—against the economic burden of manufacturing the surface—a low loss of milled material and a fast fabrication time.

The series 2 depth-selection tests focused on three interlocking surface patterns from series 1: a square wave (SQ), a triangular wave (TR), and a truncated triangular wave (TT). Each of these interlocking profiles was milled at four different depths (1/32in, 2/32in, 3/32in, and 4/32in), as described in the methodology section. The maximum load capacity and interface surface displacement for each profile and depth are shown in Fig. 5. Where no loss in maximum force is shown in Fig. 5, the final point of the curve is the point of sample failure.

The interlocking interface surface force and displacement results in Fig. 5 show that the division between abrupt failure and progressive reduction in capacity modes is still evident. The triangular (TR) and truncated triangular
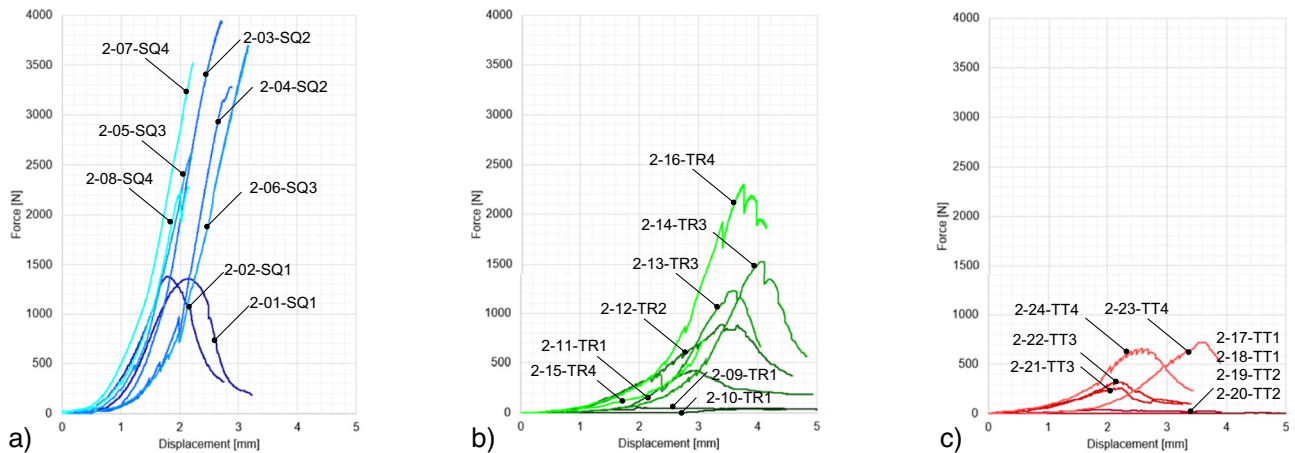
Fig. 5 | Series 2 interlocking profile depth-selection tests—load and displacement. The number following the shape code indicates the profile depth (i.e., 2-01-SQ1 refers to: series 2, test 1, square shape interlocking surface, 1/32in depth). **a** Square surface profiles, **b** triangular surface profiles, and **c** truncated triangle surface profiles.
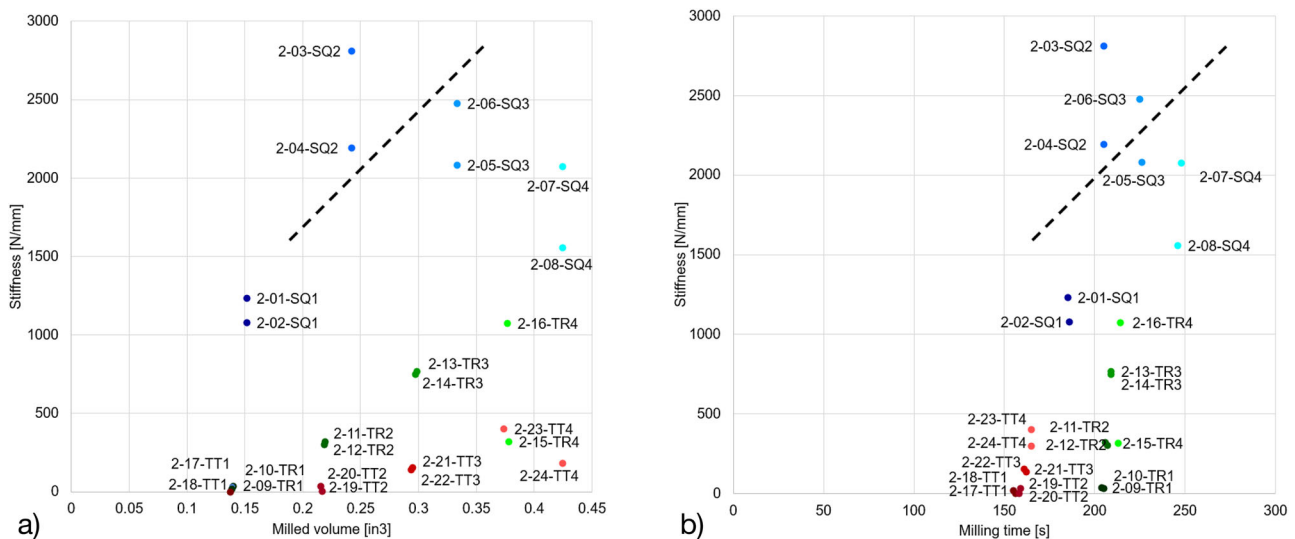
Fig. 6 | Series 2 interlocking interface surface depth-selection tests: structural performance parameters vs manufacturing performance parameters. a Relationship between stiffness and milling volume, and **b** relationship between stiffness and milling time.

(TT) profile tests exhibit progressive reduction in capacity, and a trend that indicates that the deeper the interlocking profile extends, the higher the maximum load capacity. The square (SQ) profile tests exhibited a mix of failure modes: the shallowest interlocking interface surface of 1/32in recorded progressive reduction in capacity after a peak, while all deeper interlocking interface surfaces recorded abrupt failures. The square pattern tests also did not exhibit the same trend in increased maximum load capacity with increased depth: interlocking interface surface depths between 2/32in and 4/32in all recorded maximum load capacities in a similar range between 2275 N and 3950 N.

Figure 6 plots the maximum stiffness against the milling time or volume for each test. In contrast to the series 1 tests, the variation in milling volume between the series 2 tests was larger than the variation in milling time. The maximum milling time was 60% longer than the minimum milling time, while the maximum milling volume was over 200% larger than the minimum milling volume. As with the series 1 tests, the interlocking interface surface tests with results closest to the top left corner of the charts show both good structural and manufacturing performance (indicated by the samples above the dashed line). The square profile with a depth of 2/32in (SQ2) performed best. This is the interlocking interface surface that was selected for implementation for the laminated beam in bending tests. Similar

relationships were also noted between maximum capacity and milling time, and milled volume.

Laminated beam structural performance

A high performing lamination method can be defined as one that produces a beam that balances the key performance criteria—categorized as Structural, Economic, Environmental, and Circularity—as described in Table 1.

The load-displacement results for each test, up until the maximum load the beam sustained, are shown in Fig. 7, and the full numerical results of the laminated beam tests are included in Table 2, including the mean (μ), standard deviation (σ) and coefficient of variance (CV) for each testing population. Three structural performance criteria are assessed for each beam: maximum strength, stiffness, and the type of failure mechanism.

The MOR results are grouped by lamination method to allow for a comparison of the averages of the results per method, as well as to indicate the spread of results per method (Fig. 8a). In each lamination type, there is a notable difference in load-deflection performance between the flat and grooved interfaces. The flat interfaces show an approximately linear relationship for the initial deflection period; the grooved interfaces show an approximately bilinear relationship with initially lower stiffness behavior for the first 4 mm, followed by higher stiffness behavior afterwards. This is

Fig. 7 | Laminated beam test load and displacement charts. Grooved surface interface beams shown with a dashed line, flat surface interface beams shown with a solid line. **a** GR-NG and FL-GL, **b** GR-MN and FL-MN, **c** GR-WN and FL-WN, and **d** GR-PS and FL-PS.
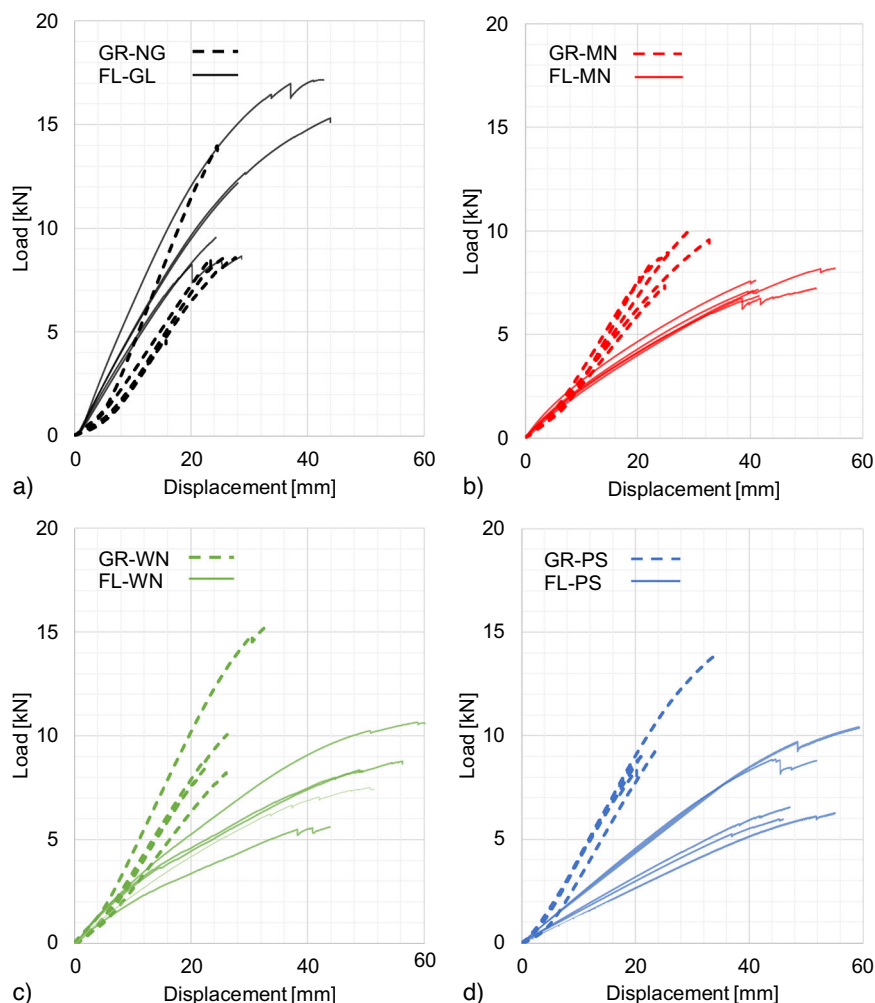
expected to be due to an initial phase of settling, where the tolerances between the interlocking groove layers are resolved (the lower stiffness behavior) before the grooves are fully engaged, producing a high stiffness interface.

With only five results in each group, the box-and-whisker representation has been selected to exclude the median from the quartile calculations. The whiskers represent the maximum and minimum results with no additional outliers; the box represents the interquartile range, with the first quartile calculated as the median of the minimum and second smallest result, and the third quartile calculated as the median of the maximum and second largest result; the line within the box represents the median; and the cross represents the mean of the five results.

The MOR results for the beam lamination methods can be grouped into three categories: lamination methods with an interlocking interface surface (GR-NG, GR-MN, GR-WN, and GR-PS), lamination methods with a non-adhesive flat interface surface (FL-MN, FL-WN, and FL-PS), and glue lamination with a flat interface surface (FL-GL). The mean and median MOR results for the interlocking interface surfaces are all larger than the mean and median MOR results for the non-adhesive flat interface surface results. If the lamination methods are compared in pairs where the same fastening method is used with both an interlocking and flat interface surface (GR-MN and FL-MN, GR-WN and FL-WN, GR-PS and FL-PS), a percentage increase in MOR between 20% and 31% can be attributed to the introduction of the interlocking interface surface (Table 3). The performance of the traditional glue lamination method (FL-GL) is markedly better, showing a 31% increase compared to the mean value of the fastened

interlocking interface surfaces, and a 62% increase compared to the mean value of flat interface surfaces (Table 3).

The four interlocking interface surface lamination methods all have mean and median MOR results within a close range, indicating that the introduction of fasteners does not provide a marked increase in capacity in addition to the interlocking interface surface. The absolute spread of MOR results for the interlocking interface surfaces was larger than for the non-adhesive flat interface surfaces. However, the glue laminated flat interface surface had the largest overall range and interquartile range of MOR results, possibly resulting from fabrication inconsistencies in sample production as indicated in Table 4.

The MOE results are grouped by lamination method to allow for a comparison of the averages of the results per method, as well as to indicate the distribution of grain orientation results per method (Fig. 8b). The same box-and-whisker calculation method was used as was described for the MOR results of Fig. 8a. It is noted that the MOE was calculated using the portion of the force-displacement curve between 20% and 40% of maximum load and therefore does not refer to the initial lower stiffness behavior of the beam prior to the grooves engaging across the interlocking surface. The MOE results for the beam lamination methods can be grouped into the same three categories as for the MOR results: lamination methods with an interlocking interface surface (GR-NG, GR-MN, GR-WN, GR-PS), lamination methods with a non-adhesive flat interface surface (FL-MN, FL-WN, and FL-PS), and glue lamination with a flat interface surface (FL-GL). The mean and median MOE results for the interlocking interface surfaces are all significantly larger than the mean and median MOR results for the non-adhesive flat interface surface. If the lamination methods are compared in

Table 2 | Table of laminated beam test results by interface surface and fastener type

Fastener type	Interface type															
	Flat (FL)								Interlocking (GR)							
Adhesive (GL)	FL-GL								GR-NG							
Tag	01	02	03	04	05	μ	σ	CV	01	02	03	04	05	μ	σ	CV
P_{max} [kN]	9.6	17.2	15.3	12.2	8.7	12.6	3.3	26%	8.6	8.6	8.6	4.6	14.0	8.9	3.0	34%
Δ_{mid} [mm]*	27.8	48.6	50.5	32.2	33.0	38.4	9.3	24%	29.2	26.8	31.7	17.9	28.1	26.8	4.7	18%
MOR [MPa]	27.7	49.8	44.4	35.3	25.1	36.5	9.5	26%	24.8	24.9	24.9	13.4	40.5	25.7	8.6	34%
MOE [GPa]	5.6	7.9	6.2	6.2	5.7	6.3	0.8	13%	5.2	4.9	5.1	3.9	8.7	5.5	1.6	30%
Metal nails (MN)	FL-MN								GR-MN							
Tag	01	02	03	04	05	μ	σ	CV	01	02	03	04	05	μ	σ	CV
P_{max} [kN]	7.2	8.2	7.6	6.9	7.2	7.4	0.5	6%	8.4	9.6	7.4	9.0	10.1	8.9	1.0	11%
Δ_{mid} [mm]*	59.4	63.3	47.0	47.8	47.6	53.0	6.9	13%	25.4	37.6	28.5	29.0	33.8	30.9	4.3	14%
MOR [MPa]	21.0	23.8	22.1	19.9	20.8	21.5	1.3	6%	24.3	27.8	21.3	26.0	29.4	25.8	2.8	11%
MOE [GPa]	2.3	2.3	2.8	2.5	2.5	2.5	0.2	6%	5.3	4.1	3.9	5.0	4.8	4.6	0.5	12%
Wood nails (WN)	FL-WN								GR-WN							
Tag	01	02	03	04	05	μ	σ	CV	01	02	03	04	05	μ	σ	CV
P_{max} [kN]	5.6	8.8	8.3	10.9	7.5	8.2	1.7	21%	10.1	8.2	15.2	8.7	8.0	10.0	2.7	27%
Δ_{mid} [mm]*	50.9	64.6	56.9	79.6	58.2	62.0	9.8	16%	30.1	29.9	37.3	26.6	24.4	29.7	4.4	15%
MOR [MPa]	16.3	25.5	24.1	31.7	21.8	23.9	5.0	21%	29.2	23.9	44.0	25.2	23.1	29.1	7.8	27%
MOE [GPa]	2.2	2.7	2.8	3.0	2.5	2.7	0.3	11%	5.55	4.35	7.07	5.38	4.91	5.45		
Plastic straps (PS)	FL-PS								GR-PS							
Tag	01	02	03	04	05	μ	σ	CV	01	02	03	04	05	μ	σ	CV
P_{max} [kN]	6.3	6.6	6.0	10.4	8.9	7.6	1.7	23%	9.3	9.0	13.8	8.4	9.3	10.0	2.0	20%
Δ_{mid} [mm]*	63.3	54.1	51.9	68.1	51.3	57.8	6.7	12%	27.4	24.8	38.8	23.2	24.7	27.8	5.7	20%
MOR [MPa]	18.2	19.0	17.3	30.3	25.7	22.1	5.0	23%	27.0	26.2	40.1	24.3	26.9	28.9	5.7	20%
MOE [GPa]	1.6	1.9	1.8	2.7	2.8	2.2	0.5	22%	5.7	6.0	6.3	5.7	5.6	5.8	0.3	4%

Fig. 8 | Box-and-whisker plots representing the mechanical property test results for each lamination method based on five results. The whiskers represent the maximum and minimum, the box represents the interquartile, the line within the box represents the median, and the cross represents the mean. **a** MOR of each beam lamination method and **b** MOE of each beam lamination method.
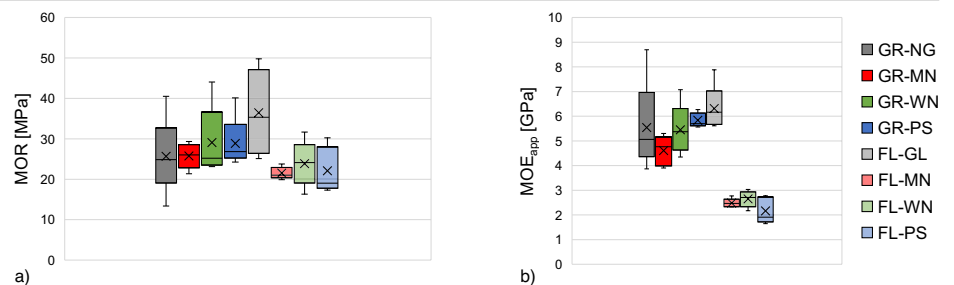
pairs where the same fastening method is used with both an interlocking and flat interface surface (GR-MN and FL-MN, GR-WN and FL-WN, GR-PS and FL-PS), a percentage increase in MOE between 86% and 170% can be attributed to the introduction of the interlocking interface surface (Table 3). The performance of the traditional glue lamination method (FL-GL) is similar to the interlocking interface surfaces, with a mean MOE 19% higher than the mean of all three interlocking interface methods. This indicates that, for beams which are controlled by stiffness instead of strength, the use of interlocking interface surfaces with non-adhesive fasteners between laminations could provide an equal or improved structural performance as compared to glue laminated beams. However, the glue lamination method is markedly better than the other fastener types for flat interface surfaces, showing a 159% increase compared to the mean value of the flat interface surfaces (Table 3). This suggests that the interlocking interface surface is

crucial in generating sufficient shear transfer between the laminations for stiff beams.

The four interlocking interface surface lamination methods all have mean and median MOE results within a small range, however, there is more variation in MOE between these lamination methods than between MOR. This indicates that the introduction of different fastener types can generate different stiffnesses when combined with the interlocking interface surface. The spread in MOE with the different fastener types is notable, with very little variation in MOE results for metal nail and plastic strap fasteners (GR-MN and GR-PS) compared to wood nails or no fastener (GR-NG and GR-WN).

The absolute spread of MOE results for the interlocking interface surfaces was larger than for the non-adhesive flat interface surfaces, which all had a smaller maximum range. The glue laminated flat interface surface

Table 3 | Difference in mean MOR and MOE for each beam lamination method pair

Fastener type	MOR [MPa]				MOE [GPa]			
	Interlocking (GR)	Flat (FL)		%	Interlocking (GR)	Flat (FL)		%
Metal nails (MN)	25.76	21.52	–	+20	4.61	2.48	–	+86
Wood nails (WN)	29.09	23.88	–	+22	5.45	2.65	–	+106
Plastic straps (PS)	28.89	22.11	–	+31	5.84	2.16	–	+170
Glue (GL)	–	–	36.47	–	–	–	6.31	–
Average	27.91	–	*36.47*	+31	5.30	–	*6.31*	+19
	–	22.50	*36.47*	+62	–	2.43	*6.31*	+159

The italic values are a duplication of the Glue (GL value). They are shown here to indicate that the % change is a comparison between the average of the second and third columns with this fourth column value.

Table 4 | Laminated beam fabrication data

Fastener type	Interface type (n_{total} = 40)									
	Flat (FL) (n_{fl} = 20)					Interlocking (GR) (n_{gr} = 20)				
Adhesive (GL)	($n_{fl,ad}$ = 5)					($n_{gr,ng}$ = 5)				
Tag	FL-GL-1	FL-GL-2	FL-GL-3	FL-GL-4	FL-GL-5	GR-NG-1	GR-NG-2	GR-NG-3	GR-NG-4	GR-NG-5
Glue volume [in3]	26	15	7.5	15	15	–	–	–	–	–
Clamping time [h]	12	4	4	4	4	–	–	–	–	–
Metal nails (MN)	($n_{fl,mn}$ = 5)					($n_{gr,mn}$ = 5)				
Tag	FL-MN-1	FL-MN-2	FL-MN-3	FL-MN-4	FL-MN-5	GR-MN-1	GR-MN-2	GR-MN-3	GR-MN-4	GR-MN-5
Nailing pattern	A	A	A	A	A	B	C	C	C	C
Wood nails (WN)	($n_{fl,wn}$ = 5)					($n_{gr,wn}$ = 5)				
Tag	FL-WN-1	FL-WN-2	FL-WN-3	FL-WN-4	FL-WN-5	GR-WN-1	GR-WN-2	GR-WN-3	GR-WN-4	GR-WN-5
Nailing pattern	A	A	A	A	A	B	C	C	C	C
Plastic straps (PS)	($n_{fl,ps}$ = 5)					($n_{gr,ps}$ = 5)				
Tag	FL-PS-1	FL-PS-2	FL-PS-3	FL-PS-4	FL-PS-5	GR-PS-1	GR-PS-2	GR-PS-3	GR-PS-4	GR-PS-5
Strap spacing [in]	3	3	3	3	3	8.5	8.5	8.5	8.5	8.5

The table lists specifics on nail patterns (see Fig. 19), fastener spacing and glue volume / glueing time for each lamination method.

had the largest overall range and interquartile range of MOE results, indicating less predictability in structural behavior.

The laminated beam test failure mechanisms can be grouped into four categories: (1) composite bending failure with tension failure at a knot in the bottom lamination; (2) composite bending failure with tension failure of the fibers in the bottom lamination; (3) non-composite bending failure, where both the top and bottom lamination fail; and (4) shear failure along some of the interface surface, either through failure of the interlocking surface or deformation of the fasteners. These failure mechanisms are shown schematically and through example photographs in Fig. 9. The observed failure mechanism of each laminated beam test is noted in Table 5.

The distribution of failure modes among the lamination methods demonstrates a clear difference in behavior between the non-adhesive flat interface surfaces (FL-MN, FL-WN, and FL-PS) and the other methods. The non-adhesive flat interface surfaces exhibited a minimum of three out of five failures through non-composite moment failure in the two laminations. This non-composite behavior aligns well with the reduced MOR and MOE for these lamination methods when compared to glue lamination (FL-GL) and the interlocking interface surfaces. The third glue lamination specimen exhibited a non-composite failure, indicating slip between the two laminations. This specimen was the beam laminated with the least volume of glue as noted in Table 4.

The interlocking interface surfaces that did not use metal nails (GR-NG, GR-WN, GR-PS) all exhibited failure through shear of the interlocking material—visible as the wooden teeth shearing off at their root. This indicates that the increased stiffness of these

lamination methods is caused by the stiffness of the interlocking surface, which functions until failure.
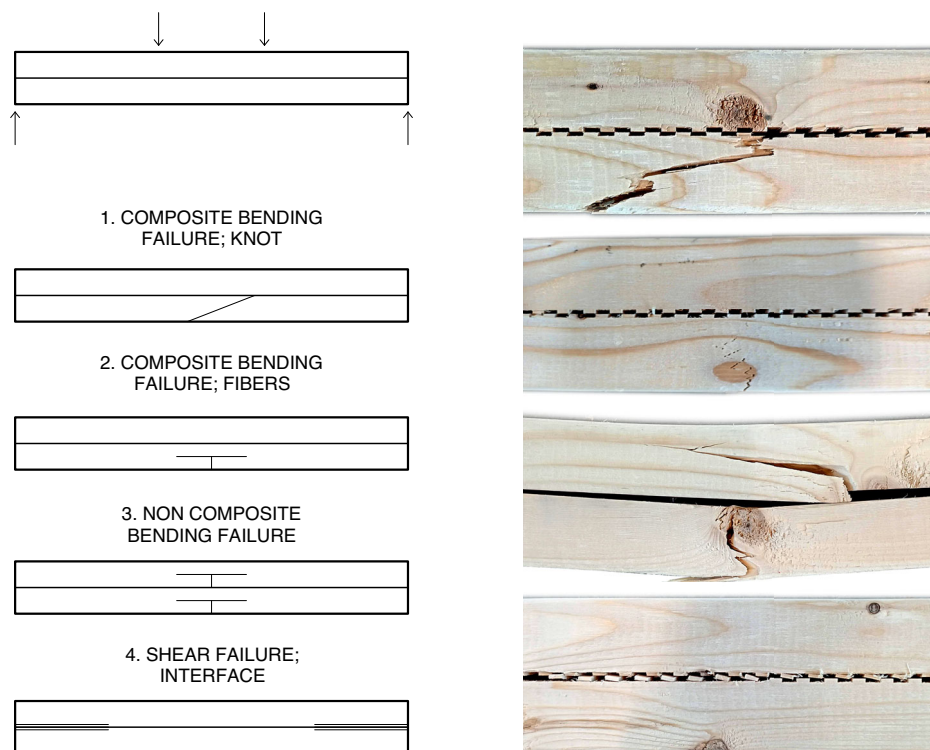
Laminated beam economic performance

The economic performance data is shown in Table 6. There is a clear premium in production time and costs for producing the beams with the interlocking lamination methods. The estimated cost of the most expensive lamination method (GR-PS) is nearly 4.5 times that of the least expensive (FL-MN).

However, the production time and cost increase in this comparison are expected to be artefacts of the university research environment, and the use of an adjustable milling process that allows for a variation in depth and spacing. CNC milling is an inefficient method for forming a regular and defined series of interlocking grooves, and at a commercial facility, this could more easily be completed using horizontal gang milling and linear movement of the lumber instead of the router head. The economic data is presented for reference; however, it is not expected to accurately represent the relative cost of future commercial manufacturing of the grooved interface beams. Therefore, it has been removed from the visual multi-factor evaluation in Fig. 10.

Laminated beam environmental performance

The environmental performance data is shown in Table 7, with the GWP data displayed in Fig. 11. The health hazards from the laminated beams are primarily limited to the impact of the adhesive used in the flat interlocking glued lamination method (FL-GL).

Fig. 9 | Bending failure mechanisms in four-point bending test. Illustrated schematically on the left and as images from series 2 beam tests on the right (same order from top to bottom).

1. COMPOSITE BENDING FAILURE; KNOT

2. COMPOSITE BENDING FAILURE; FIBERS

3. NON COMPOSITE BENDING FAILURE

4. SHEAR FAILURE; INTERFACE

Table 5 | Observed failure mechanism for each beam

Interface type	Fastener type	Specimen				
		1	2	3	4	5
GR	NG	4	1	4	1	4
	MN	2	1	2	1	2
	WN	1	1	4	4	1
	PS	1	4	4	1	1
FL	GL	1	4	3	2	1
	MN	1	3	3	3	1
	WN	1	3	3	3	3
	PS	3	3	3	1	3

Failure mechanisms are illustrated in Fig. 9 and numbered as follows: 1. Composite Bending Failure: Knot; 2. Composite Bending Failure: Fibers; 3. Non Composite Bending Failure; 4. Shear Failure: Interface.

The GWP results in Fig. 11 are for cradle-to-site embodied carbon emissions, and exclude emissions associated with the energy usage of the machines associated with manufacture in the shop. Figure 11 shows a near-constant contribution associated with the wood used to fabricate the beams—approximately evenly split between the A1–A3 modules for material extraction and processing, and the A4 module delivery from the sawmill to the fabrication facility. This high GWP contribution from transportation is associated with the specific sawmill in Quebec, where the wood for the project was sourced by the local builder's merchant. A4 transport emissions for the fasteners are negligible due to their relatively small weight and volume. There is a notable difference in the A1–A3 emissions between the plastic strap fasteners and adhesive when compared to the metal and wood nails. However, these A1–A3 impact numbers are sensitive to the specificities of the material type and sources, and local EPDs for both plastic straps and wood resins are not widely available. The PVAc value used in this assessment is close to the average of the value of a 65% solids MUF resin and 65% solids MF resin[53]. The resulting A1–A3 percentage increase between glulam (FL-GL) and wood with no fasteners (GR-NG) is 56%, which is less

than the difference between the North American benchmarks for lumber and glulam produced by the American Wood Council and Canadian Wood Council of 117% and between the Canadian benchmarks for lumber and glulam of 240%[53]. This indicates that the estimation of the embodied carbon emissions for glulam in the laboratory process is a lower bound and may be missing other commercial lamination processes. EPDs for plastic strap cable ties are uncommon, and values for the source material nylon 6/6 vary significantly, subject to the reporting sources. However, the use of an average value from a national aggregated database was deemed appropriate. It is also noted that nylon cable ties were used for this study as opposed to steel straps due to the small dimensions of the cross-section. If larger beam cross-sections were fabricated, then steel straps could be used. The impact of this change on the environmental performance evaluation would then need to be assessed.

Considering the potential for some variability in the environmental impact of both the strap material and adhesive, the trend is clear that the use of these more-intensive fasteners can lead to an approximately 50% increase in GWP for the interlocking plastic straps (GR-PS) and conventional glulam (FL-GL) when benchmarked against the metal and wood nail interlocking solutions (GR-MN, GR-WN), and a 130% increase when comparing the flat interface plastic strap solution against the metal and wood nail interlocking solutions (GR-MN and GR-WN).

Laminated beam circularity performance

The qualitative circularity performance assessment results are shown in Table 8, divided into aspects of processing and end-of-life scenarios by lamination method. The barriers to future processing are related to the fastener type and material: nails and adhesives are irreversible, while metal and plastic are non-machinable with conventional woodworking tools. Some of these fasteners can be removed to allow for future machining—such as metal nails and plastic fasteners—although the removal of metal nails is currently a high-effort process requiring labor and/or advanced robotic technology. The wood nails and adhesive lamination system are not reversible, but they are machinable (it is in principle feasible to rip glulam along the laminated glue lines to separate the laminations). This means that the process used to gain utility from laminating wood using these systems

Table 6 | Economic performance data per beam lamination method per foot of beam

Interface type	Fastener type	Waste	Production			Cost			
		Wood [%]	Milling [s]	Fabrication [s]	Total [s]	Beam [$]	Fasteners [$]	Fabrication [$]	Total [$]
GR	NG	6.7	1186	1	1187	0.86	0.00	5.27	6.13
	MN	6.7	1186	42	1228	0.86	0.10	5.46	6.42
	WN	6.7	1186	42	1228	0.86	0.38	5.46	6.70
	PS	6.7	1186	75	1261	0.86	0.47	5.60	6.93
FL	GL	4.4	20	107	127	0.86	0.55	0.56	1.98
	MN	0.0	0	80	80	0.86	0.27	0.336	1.49
	WN	0.0	0	56	56	0.86	1.04	0.25	2.15
	PS	0.0	0	193	193	0.86	1.28	0.86	3.00

Fig. 10 | Global Warming Potential of lamination methods. Embodied carbon values subdivided by element and LCA modules A1-A4 per beam lamination method per foot of beam.
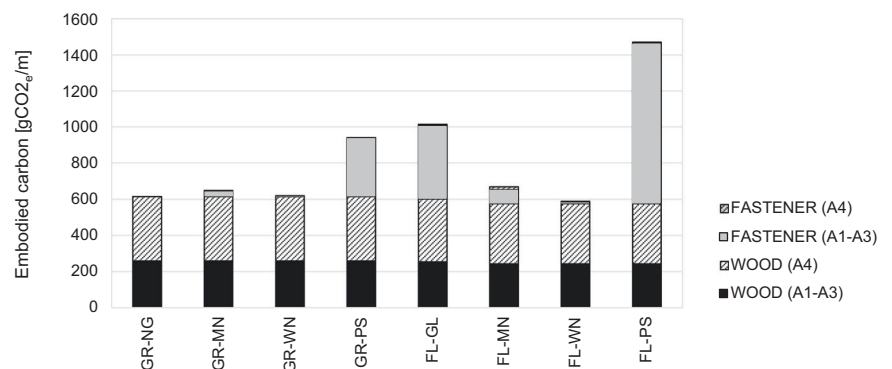
Table 7 | Environmental performance data per beam lamination method per meter of beam

Interface type	Fastener type	GWP					Health	
		Wood		Fastener		Total	VOC	Hazards
		A1–A3	A4	A1–A3	A4	A1–A4		
		[gCO2e]	[gCO2e]	[gCO2e]	[gCO2e]	[gCO2e]	[−]	[−]
GR	NG	259	357	0	0	616	N	–
	MN	259	357	28	6	650	N	–
	WN	259	357	2	3	621	N	–
	PS	259	357	324	2	941	N	Microplastics
FL	GL	254	348	405	8	1015	Y	Carcinogen, Asthmagen
	MN	243	334	77	17	670	N	–
	WN	243	334	6	7	590	N	–
	PS	243	334	890	5	1471	N	–

does not restrict future reprocessing as an alternative structural element. The aggregated total for end-of-life scenarios is similar for most lamination methods, with an approximate 50% rating performance increase for the lamination methods that are mono-material systems that use either no fastener, or wood fasteners.

**Laminated beam overall performance**

The overall performance of each criterion by subcategory is shown in Table 9. The average value for each of the three relevant criteria—structure, environment, and circularity—is shown in a radar plot in Fig. 10. The dashed lines indicate the grooved interface surfaces, and the solid lines indicate the flat interface surfaces. The economic criterion is obscured in visual comparison as the data is highly associated with the laboratory

manufacturing process as opposed to the potential commercial process. No lamination method performs best in all three criteria. The conventional glulam (FL-GL) has the highest structural rating (5.0), but poor environmental and circularity ratings (0.1 and 1.3) associated with the irreversible, toxic, and emission-intensive manufacture of the adhesive.

All the interlocking systems (GR-) perform at an intermediate rating in the structural criterion (between 2.1 and 3.4), but the environmental rating of the interlocking systems with plastics straps is low (GR-PS, rating 2.0) compared to the metal and wood fastener systems (GR-MN, rating 4.8; GR-WN, rating 4.9) due to the emission-intensive manufacture of the nylon material. The circularity ratings are highest for the systems that use either no fastener (GR-NG, rating 5.0) or the mono-material wood nails (GR-WN, rating 3.4).

Fig. 11 | Multi-factor performance criteria comparison. Radar chart indicating relative performance of the lamination methods against the criteria of Structure, Environment and Circularity. Dashed lines indicate grooved interface surfaces, solid lines indicate flat surface interfaces.
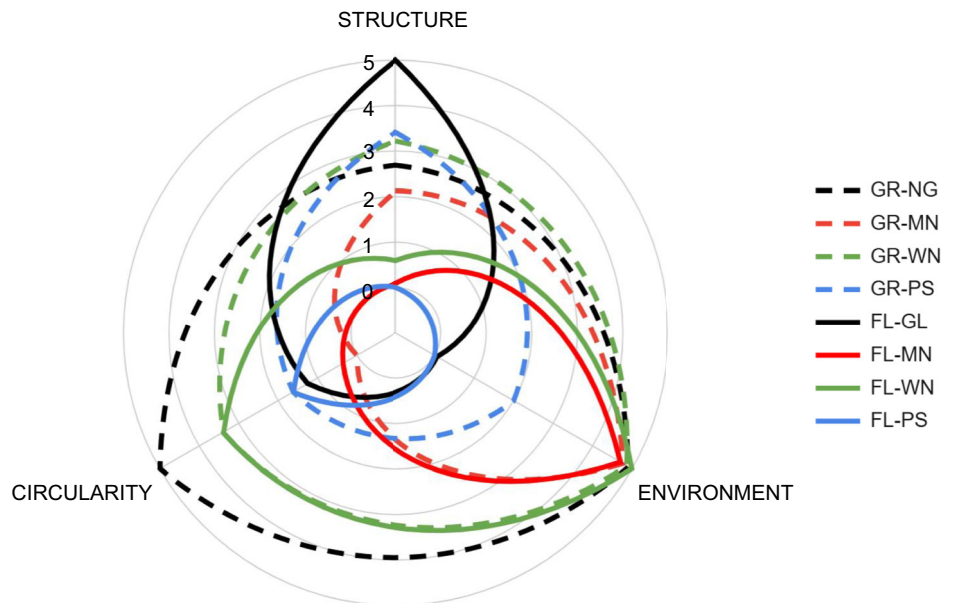
Table 8 | Circularity performance data per beam lamination method per foot of beam (ratings between 0 (min) and 5 (max))

Interface type	Fastener type	Processing		End-of-life scenarios				
		Reversible	Machinable	Reuse	Remanu-facture	Recycle/ Compost	Incineration/landfill	Total
GR	NG	Y	Y	5	4	5	5	19
	MN	N	N	5	1	2	4	12
	WN	N	Y	5	3	5	5	18
	PS	Y	N	4	4	3	2	13
FL	GL	N	Y	5	5	0	2	12
	MN	N	N	5	2	2	4	13
	WN	N	Y	5	3	5	5	18
	PS	Y	N	3	5	3	2	13

Table 9 | Multi-factor performance criteria ratings comparison table

Interface type	Fastener type	Structure			Economy				Environment			Circularity		
		Strength	Stiffness	μ	Waste	Production	Cost	μ	GWP	Health	μ	Reprocessing	End of life	μ
GR	NG	1.4	4.1	2.7	0.0	0.3	0.7	0.3	4.9	5.0	4.9	5.0	5.0	5.0
	MN	1.4	3.0	2.1	0.0	0.1	0.5	0.2	4.7	5.0	4.8	0.0	0.0	0.0
	WN	2.5	4.0	3.2	0.0	0.1	0.2	0.1	4.8	5.0	4.9	2.5	4.1	3.4
	PS	2.5	4.4	3.4	0.0	0.0	0.0	0.0	3.0	2.5	2.0	5.0	4.1	1.6
FL	GL	5.0	5.0	5.0	1.7	4.7	4.6	3.7	2.6	0.0	0.1	2.5	0.6	1.3
	MN	0	0.4	0.1	5.0	4.9	5.0	5.0	4.5	5.0	4.7	0.0	0.0	0.4
	WN	0.8	0.6	0.6	5.0	5.0	4.4	4.8	5.0	5.0	5.0	2.5	2.6	3.4
	PS	0.2	0.0	0.0	5.0	4.4	3.6	4.4	0.0	2.5	0.0	5.0	4.7	1.6

Reviewing all three criteria in parallel allows us to assess the lamination methods on a holistic level and filter the eight lamination methods to two viable, best-performing methods: the highest structurally performing lamination method (conventional glulam, FL-GL) and the best alternative lamination method. Of the interlocking interface methods, the no glue (GR-NG) performs the best in circularity and environmental criteria, however, this method is considered a non-viable benchmark system—the lack of any fastening system between layers would make fabrication, transportation, and installation exceptionally challenging. Additionally, the presence of fasteners prevents the opening of gaps between the laminations under peeling stress. The second-best alternative lamination method for circularity and environment is the two wood nail systems (GR-WN and FL-WN), while the interlocking wood nail system has a higher structure rating of the two.

Discussion

This study suggests that the grooved interlocking interface fastened with wood nails (GR-WN, herein referred to as *GrooveLam*) is a good circular

and environmental alternative wood lamination method to conventional glulam (FL-GL). However, the results of this study require further development to demonstrate the suitability of this alternative lamination method at scale. This future research could primarily follow three tracks, based on: element dimension, commercial manufacturing, and regulatory barriers.

The current study was limited to short beam elements formed of two laminations, and where each lamination was a continuous piece of lumber. To produce elements at the structural depth required for use in the construction of buildings, four or more laminations would be necessary within a beam cross-section. This will require exploring the manufacturing processes of forming interlocking interfaces on both faces of the interior laminations and defining a suitable fastener layout and fastening sequence that provides a suitable connection between laminations without interference between fasteners. Research on this topic is currently ongoing. The proportions and dimensions of the interlocking surfaces could be maintained the same as for this study for elements' cross sections with more laminations, as the wood feedstock for the single lamination layers was a similar thickness to that which would typically be used for multi-lamination beams.

To produce elements at the structural length required for use in the construction of buildings, elements would typically be over 3.7 m (12 feet) in length. For shorter structural spans, it is feasible that long single pieces of lumber could be used, however, for longer elements, individual lumber feedstock would need to be connected end-to-end. In conventional glulam, these connections are achieved with glued finger joints. To maintain a mono-material wood-only element in line with the lamination method, it is proposed that alternative methods for connecting lumber end-to-end, such as dovetail connections, could be tested. Research on this topic is currently ongoing.

The structural widths of elements are limited only by the depth of the lumber feedstock. Structural dimension elements can be manufactured with 2×4 lumber, and for larger beams, 2×6 and 2×8 lumber could also be considered. Therefore, lamination of feedstock across the width of the element is not necessarily anticipated for exploration.

The current study highlighted limitations in the economic evaluation between manufacturing GrooveLam and glulam within the facilities available at the architecture department. Future research proposes a partnership with commercial fabricators to conduct a larger-scale fabrication, where the manufacturing process can be refined, and economic subcategory values can be more reliably recorded. The refinement of this process would focus on an improved method of forming the interlocking grooves. Research on this topic is currently ongoing.

Additional commercial research questions are to determine which project types would specifically benefit from GrooveLam as opposed to glulam EWP elements. Environmentally focused projects that seek to limit the use of fossil fuel-derived products or health-focused projects that seek to limit the presence of non-natural VOCs are considered suitable typologies. Research on this topic is currently ongoing.

The bilinear behavior of the grooved lamination method beam results —with an initial low-stiffness period before the grooved interfaces fully engage—will need to be further reviewed in future research to allow for fabricators and designers to accommodate this behavior in structures. It is envisaged that this could be through tighter manufacturing tolerances, the application of a preload prior to fastening across the laminations, or other methods to account for this initial displacement through design, as with beam precamber.

The current study focused on the structural, circular, and environmental performance of the lamination methods. However, other factors would likely require exploration to satisfy the regulations that are applied to glulam, such as the comparative performance of GrooveLam under fire-loading scenarios compared to glulam, or regarding requirements for reclaimed lumber prior to application in GrooveLam for code compliance in structural applications. Experiments on both research questions are currently ongoing.

Commercial manufacturing of GrooveLam will require reliable and consistent supplies of reclaimed lumber, sourced from the built

environment in proximity to fabrication and reapplication. This condition requires the development of a suitable economic and regulatory framework, which is further discussed in Heisel et al. [43].

EWPs constitute a diverse range of structural element types and are attractive from an environmental perspective. However, the use of adhesive resins can limit the ability of the elements to perform within a circular economy, and the glue-laminating process reduces the environmental performance of many EWPs when compared to the source wood feedstock. This research demonstrated that alternative lamination methods featuring an enhanced longitudinal shear transfer mechanism between individual laminations can produce beam elements with comparable structural performance to adhesive lamination for flat elements, and improved circular and environmental performance.

This research demonstrated the variable performance of the shape of the interlocking pattern, and determined an optimal interlocking pattern of square grooves at a 1/16in depth that balanced structural performance with manufacturing time and material use considerations. A multi-factor evaluation of different non-adhesive fastening methods indicated that the most promising alternative beam fabrication to conventional glulam was the use of pneumatically installed lignin-welded wood nails to fasten wood feedstock milled with the interlocking interface surface (GrooveLam).

A glulam beam benchmark demonstrated a 31% increase in MOR and a 19% increase in MOE compared to beams with a combination of mechanical fasteners and an interlocking interface surface. These results were significantly closer than glulam beams when compared to beams with mechanical fasteners and a flat interface surface, where glulam had a 62% increase in MOR and a 159% increase in MOE. The environmental performance evaluation favored lamination methods that avoid embodied carbon-intensive materials such as resins and plastics, and the circularity performance evaluation favored beams fabricated entirely of wood, which facilitate reprocessing and a low-impact end of life.

Future research will explore the technical challenges involved in fabricating and testing multi-lamination beam cross-sections of 200 mm (8 inches) and deeper, and fabricating beams at structural lengths of 3.7 m (12 feet) and longer. These technical challenges should be explored in parallel to a review of the implications of scaling fabrication from the research context to commercial fabrication facilities and developing supporting practical guidance for specifying GrooveLam to overcome key design challenges and to fit within the existing regulatory framework of building codes and standard design practice.

Methods
Interlocking surface samples in shear

A shear transfer mechanism is required to prevent sliding between two wood elements that share an interface surface that is parallel to an applied force (Fig. 12). If no mechanical fasteners or adhesives connect the two wood elements across this interface surface, shear transfer can only be generated by friction. The friction force F at the interface surface between the two elements is the product of the force perpendicular to the surface R, and the friction coefficient between the surfaces μ (Eq. 1).

$$F = \mu \cdot R \qquad (1)$$

Equation 1—*Friction force*.

To increase the shear resistance of the assembly, either an increase in the friction coefficient between the wood elements, or an increase in the perpendicular force is required. Wood is an anisotropic material with a lower resistance to load applied perpendicular to the direction of the grain than parallel to the grain. In cases where the grain of the wood is parallel to the interface surface, the shear resistance through friction between the wood elements is limited by crushing of the wood perpendicular to the grain due to an increase in force R. An increase in friction coefficient could increase the shear resistance of the assembly without reaching the wood crushing limit. Instead of improving the friction coefficient on the micro scale, a macro

Fig. 12 | Typical shear interlocking sample.
a Annotated dimensions and **b** shear resistance
diagram between two wood elements.
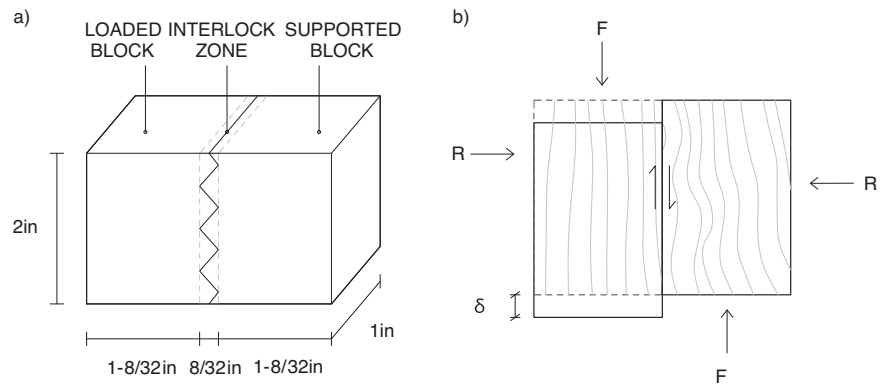
Table 10 | Series 1 shear interlocking sample fabrication data

Test #	Test shape name	Short name	Interlocking zone [in]	Wavelength [in]	Milling time [s]	Milled volume [in³]
1-01	NO INTERLOCK	1-01-FLAT	8/32	-	N/A	N/A
1-02	STEPPED	1-02-STEP	8/32	2	354.0	0.344
1-03	STEPPED	1-03-STEP	8/32	2	350.0	0.281
1-04	SQUARE (NARROW)	1-04-SQ-N	8/32	1/2	331.0	0.313
1-05	SQUARE (NARROW)	1-05-SQ-N	8/32	1/2	331.0	0.313
1-06	SQUARE (WIDE)	1-06-SQ-W	8/32	1	264.5	0.313
1-07	SQUARE (WIDE)	1-07-SQ-W	8/32	1	264.5	0.313
1-08	TRIANGLE (NARROW)	1-08-TR-N	8/32	1/4	516.0	0.313
1-09	TRIANGLE (NARROW)	1-09-TR-N	8/32	1/4	516.0	0.313
1-10	TRIANGLE (WIDE)	1-10-TR-W	8/32	1/2	256.0	0.313
1-11	TRIANGLE (WIDE)	1-11-TR-W	8/32	1/2	256.0	0.313
1-12	TRUNCATED TRIANGLE (NARROW)	1-12-TT-N	8/32	1/2	242.5	0.313
1-13	TRUNCATED TRIANGLE (NARROW)	1-13-TT-N	8/32	1/2	242.5	0.313
1-14	TRUNCATED TRIANGLE (WIDE)	1-14-TT-W	8/32	1	459.5	0.313
1-15	TRUNCATED TRIANGLE (WIDE)	1-15-TT-W	8/32	1	459.5	0.313
1-16	PYRAMIDAL	1-16-PYRA	8/32	1/2	712.0	0.417
1-17	PYRAMIDAL	1-17-PYRA	8/32	1/2	860.0	0.208

scale approach is explored through milling the two wood elements to create an interlocking shear surface. Compared to a flat surface, an interlocking surface improves the shear transfer between elements. The exact influence of the shape and depth of the interlocking surface needed to be determined through testing.

Interlocking sample fabrication
To test the influence of shape and depth, shear interlocking samples were fabricated. Varying interlocking surface profiles were cut into 2 in × 1 in × 1-28/32in blocks (height, thickness, width). The combined total wood volume before milling for each combined test sample was 7.5 in³. The combined fabricated interlocking samples—including both wood elements interlocked—varied in total size subject to the width of the interlocking zone, from 2 in × 1 in × 3-16/32 in (8/32 in interlocking zone) to 2 in × 1 in × 3-23/32 in (1/32 in interlocking zone) (Fig. 12 and Tables 10 and 11).

The samples were fabricated and tested in two sample series. The number of tested specimens was too low to allow for statistically significant conclusions, but provided an indicative comparison between different interlocking shapes and depths. The first series—exploratory tests—focused on the influence of the interlocking surface profile and wavelength (the distance for the profile to repeat) and contained 17 samples of six different patterns. The first series was fabricated from an old-growth hard pine population reclaimed from the Catherine Commons Deconstruction project, whose mechanical properties were evaluated as part of the Circulating Matters installation[18]. The interlocking surface profiles and sample fabrication data (milling time and milled material volume) are described in Fig. 13 and Table 10.

The second series—depth-selection tests—focused on the influence of the depth of the interlocking surface profile and contained 24 samples of three different patterns with four unique interlocking depths considered per shape. The same pattern wavelength of 0.5in was used for all samples. The second series was fabricated from stud-grade SPF dimensional lumber. The interlocking surface profiles and sample fabrication data (milling time and milled material volume) are described in Fig. 14 and Table 11.

The interlocking surface profiles were milled into the surface of the lumber using a CNT-950 series CNC machine with a positioning accuracy of ±0.002in and then sawn into 2in long testing sections. The specification of reclaimed wood for the first series was to demonstrate the potential circularity of the process. The use of different materials for the first and second test series means that the results can only be compared within the same series, and not between series.

Interlocking sample testing rig
To study the comparative effect of the different shear interlocking profiles on the shear resistance of the samples requires a test which would record

**Table 11 | Series 2 shear interlocking sample fabrication data**

Test #	Test shape name	Short name	Interlocking zone [in]	Milling time [s]	Milled volume [in³]
2-01	SQUARE 1/32	2-01-SQ1	1/32	185	0.151
2-02	SQUARE 1/32	2-02-SQ1	1/32	186	0.151
2-03	SQUARE 2/32	2-03-SQ2	2/32	205	0.242
2-04	SQUARE 2/32	2-04-SQ2	2/32	205	0.242
2-05	SQUARE 3/32	2-05-SQ3	3/32	226	0.333
2-06	SQUARE 3/32	2-06-SQ3	3/32	225	0.333
2-07	SQUARE 4/32	2-07-SQ4	4/32	248	0.425
2-08	SQUARE 4/32	2-08-SQ4	4/32	246	0.425
2-09	TRIANGLE 1/32	2-09-TR1	1/32	204	0.140
2-10	TRIANGLE 1/32	2-10-TR1	1/32	205	0.140
2-11	TRIANGLE 2/32	2-11-TR2	2/32	206	0.219
2-12	TRIANGLE 2/32	2-12-TR2	2/32	207	0.219
2-13	TRIANGLE 3/32	2-13-TR3	3/32	209	0.299
2-14	TRIANGLE 3/32	2-14-TR3	3/32	209	0.298
2-15	TRIANGLE 4/32	2-15-TR4	4/32	213	0.378
2-16	TRIANGLE 4/32	2-16-TR4	4/32	214	0.377
2-17	TRUNCATED TRIANGLE 1/32	2-17-TT1	1/32	155	0.139
2-18	TRUNCATED TRIANGLE 1/32	2-18-TT1	1/32	156	0.138
2-19	TRUNCATED TRIANGLE 2/32	2-19-TT2	2/32	158	0.217
2-20	TRUNCATED TRIANGLE 2/32	2-20-TT2	2/32	159	0.216
2-21	TRUNCATED TRIANGLE 3/32	2-21-TT3	3/32	161	0.295
2-22	TRUNCATED TRIANGLE 3/32	2-22-TT3	3/32	162	0.294
2-23	TRUNCATED TRIANGLE 4/32	2-23-TT4	4/32	165	0.374
2-24	TRUNCATED TRIANGLE 4/32	2-24-TT4	4/32	165	0.373
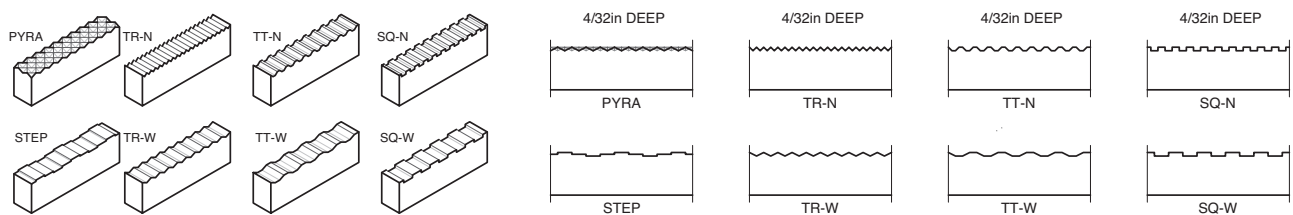
Fig. 13 | Series 1 shear interlocking sample shapes. Relative comparison representation of interlocking surfaces in axonometric view and elevation.
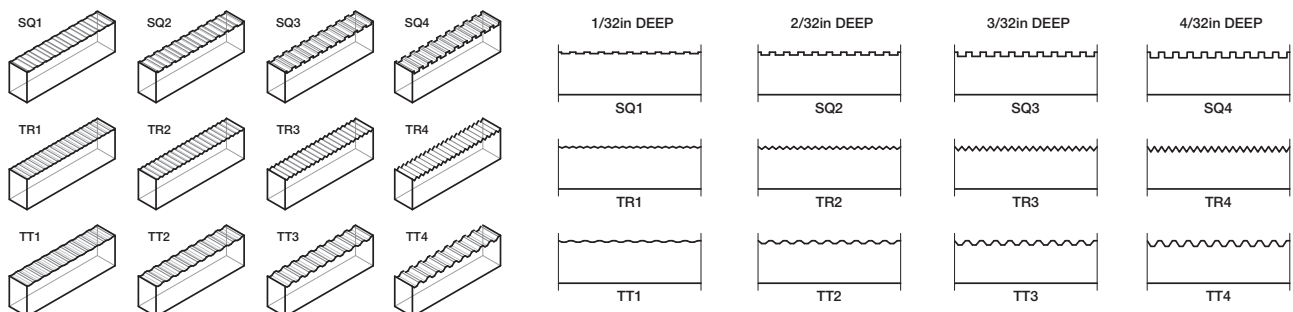
Fig. 14 | Series 2 shear interlocking sample shapes. Relative comparison representation of interlocking surfaces in axonometric view and elevation.

over time: the shearing force applied to the sample (F), the shearing displacement parallel to the interlocking surface (δ), and the clamping force applied perpendicular to the interlocking surface (R). A bespoke testing rig was designed based on adjustments of the testing rigs and sample size specified in the Shear Parallel-to-Grain Test of ASTM D143 Standard Test Methods for Small Clear Specimens[54] of Timber and ASTM D905 Standard Test Method for Strength Properties of Adhesive Bonds in Shear by Compression Loading[55] (Fig. 15). It was fabricated from a 5/8in thick carbon steel plate to bolt to the 2810-400 series 5kN capacity 4-point bending test apparatus of a model 5566 INSTRON universal testing machine (UTM)
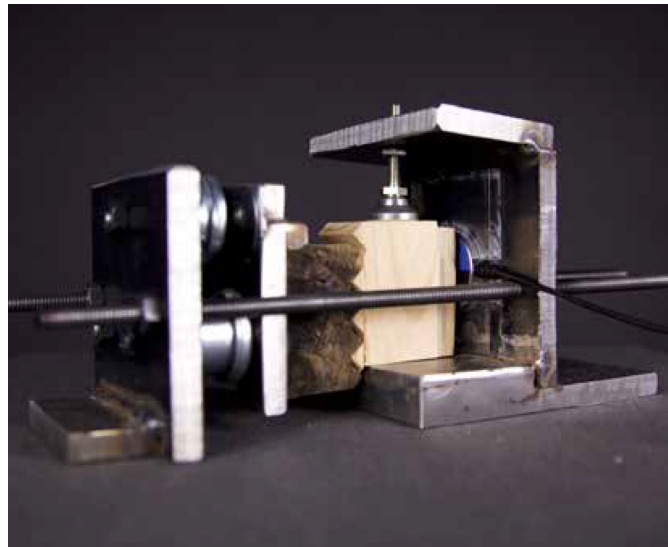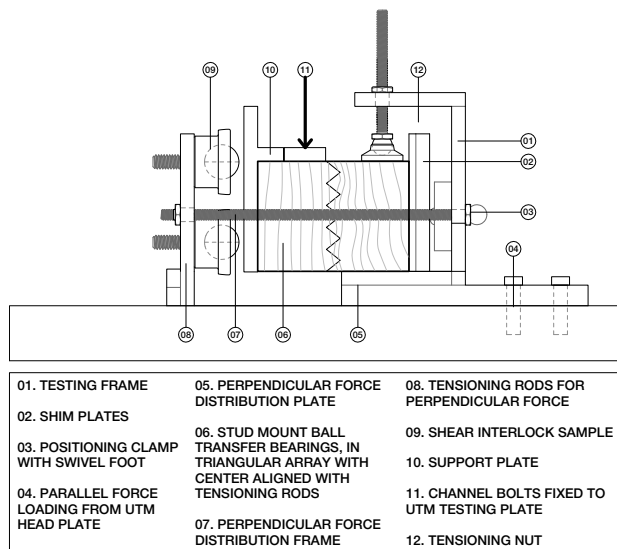
Fig. 15 | Shear interlocking sample testing apparatus. Annotated elevation and photograph of the fabricated apparatus.
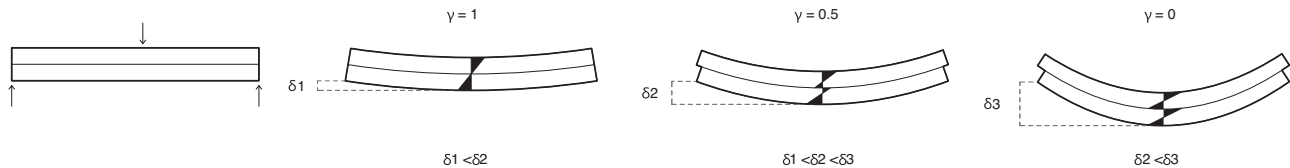
Fig. 16 | Impact of longitudinal shear transfer on strength and stiffness of two-layer laminated beams. Schematic representation of bending stress within the laminations and the relative deflection of the beam under three-point bending for three levels of inter-lamination shear transfer.

with a 2525-804 10kN capacity load cell. The use of ball transfer bearings allowed for the force perpendicular to the interlocking surface to be applied without restricting the displacement parallel to the interlocking surface. The force perpendicular to the surface was measured through a second MFD-200-050-S Loadstar Sensor 990 N (200lbf) iLoad Mini Dome capacitive load cell, located behind the sample in the test apparatus.

Interlocking sample testing protocol

Each shear test started with a target nominal preload perpendicular to the interlocking surface of 44.5 N (10lbf) ± 25% set through adjusting the sliding tensioning bar of the test apparatus. The loading head was lowered to the load distribution plate, and the test was completed with a uniform rate of loading of 1 mm/min (0.04 in/min). Changes in the perpendicular load were logged in addition to the applied shear force.

Each test was terminated after either: a loss of shear-resisting capacity, a visible failure of the interlocking surface (although shear-resisting capacity continued to increase due to a wedge effect), or a displacement of 7 mm of the loading head. The resulting logs from the UTM loading head loading and displacement parallel to the interlocking surface were then combined with the record of the load perpendicular to the interlocking surface to provide a record of the maximum shear capacity, interface shear stiffness, and the maximum load perpendicular to the interlocking surface required to support the shear resistance.

Lamination methods for beams in bending

Laminated beams connect dimensional lumber elements layered in the direction of the load. The effectiveness of the lamination method in transferring longitudinal shear between the individual layers is important in defining the strength and stiffness of the combined cross-section, with highly effective shear transfer mechanisms leading to stiffer beams with higher strength capacities than ineffective shear transfer mechanisms (Fig. 16). Mechanically Jointed Beams Theory (MJBT)[56] is a method for

calculating the strength and stiffness of mechanically laminated beams based on the stiffness of each layer and a shear transfer parameter γ that connects them (Eq. 2). The shear transfer parameter γ is a function of the spacing of the mechanical fasteners s, and the slip modulus K of mechanical fasteners (Eq. 3), as well as the length.

$$(EI)_{ef} = \sum_{i=1}^{3} (E_i I_i + \gamma_i E_i A_i a_i^2) \tag{2}$$

Equation 2—*Effective bending stiffness of a two-layer mechanically jointed beam.*

$$\gamma_i = \left[1 + \pi^2 E_i A_i s_i / (K_i l^2) \right]^{-1} \tag{3}$$

Equation 3—*Shear transfer parameter of fastening mechanism a function of fastener spacing, slip modulus, and beam length.*

Equations to predict the slip modulus are available for some specific fastener types (such as a dowel-type fastener or screw) and vary depending on specific receiving materials (timber-timber or timber-concrete) and on the reference document (manufacturer documentation, national technical standards)[57].

Existing predictive equations were developed based on empirical testing and are currently only available for commonly used fasteners in combination with flat interface surfaces. To compare the effectiveness of non-standard mechanical fasteners and non-flat interface surface treatments in transferring shear between layers in laminated beams in bending, where suitable predictive equations have not yet been developed, a series of equivalent beams was fabricated and tested in bending. The test results allow the effectiveness of the combination of fastener and interface surface treatment to be compared quantitatively for maximum failure load and
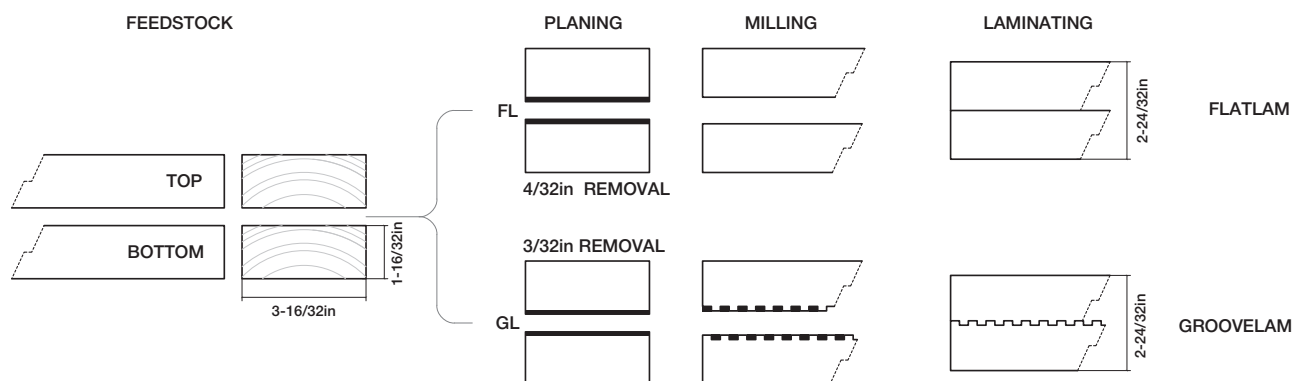
Fig. 17 | Dimensional lumber processing to form laminated beams. Process diagram showing the initial lumber dimensions, the thickness of material removed during planing, and the final dimensions of the laminated beam samples.

MOE. The load-deflection curve can also be used to qualitatively interpret the beam failure behavior.

Laminated beam specimen fabrication

Forty laminated beams were fabricated with a length of 54 in, a width of 3-1/2 in, and an overall depth of 2-3/4 in, formed of two equal-depth dimensional lumber layers. Each layer was individually fabricated from nominal 2 × 4 SPF (spruce-pine-fir, 1-1/2 in × 3-1/2 in) no. 2 grade dimensional lumber bought at Cayuga Lumber, Ithaca, NY. The lumber was selected from the lumber yard for its straight grain and minimal bow. This selection was to minimize the effect of differing natural defects in the feedstock on the comparison results between different lamination methods. This selection process is not representative of proposed future fabrication methods that would utilize a wider range of feedstock qualities within a grade class. When cutting and fabricating the laminated beam, the lumber feedstock was not selected based on the location of the knots.

The nominal 2 × 4 lumber was processed following one of two methods, subject to the interface surface treatment. The 20 laminated beams with a flat interface surface had 4/32in planed from each piece of lumber; the 20 laminated beams with an interlocking interface surface had 3/32in planed from each piece of lumber followed by milling the interlocking pattern using a CNT Motion 950 CNC router (Fig. 17). Prior to milling the interlocking pattern, an additional flat pass is completed with the routing head to regulate the level—this is to overcome any irregularities with the piece sitting on the CNC bed. This is then followed by routing the interlocking pattern with a total depth of 2/32in. To ensure that the interlocking interface surfaces mate appropriately, an additional 2/32in tolerance was milled into the interlocking pattern where the teeth meet (Fig. 18). The router was passed over the dimensional lumber across the grain using only a single pass.

A total of 40 laminated beams were tested—5 beams per combination of 4 fastener types (glue, metal nail, wood nail, plastic straps) and 2 interface surface types (flat or grooved). The matrix of combinations is shown in Fig. 2; the 40 beams are referenced Table 4. The fabrication method details for the two different interface surface treatments vary within the fastener pairs: For the flat interface surfaces, the maximum strength lamination was applied (i.e., closer spacing of fasteners), while the interlocking interface surface had a reduced lamination strength (i.e., wider spacing of fasteners)—as described in the following paragraphs in more detail. The lamination process was applied uniformly along the beam length, with no variation of fasteners between the ends and the middle of the beam.

The adhesive laminating process with the flat interface surface treatment was applied using a process based upon a conventional commercial glulam process, adjusted to guarantee a safe working environment, and with adjustments related to the clamping and spreading equipment available. Titebond Melamine glue—a specialized vinyl acetate emulsion adhesive (PVAc)—was used for fabrication as opposed to a Melamine Formaldehyde (MF) or Melamine Urea Formaldehyde (MUF) resin, as these resins can cause skin irritation from direct contact, or irritation of the eyes and upper
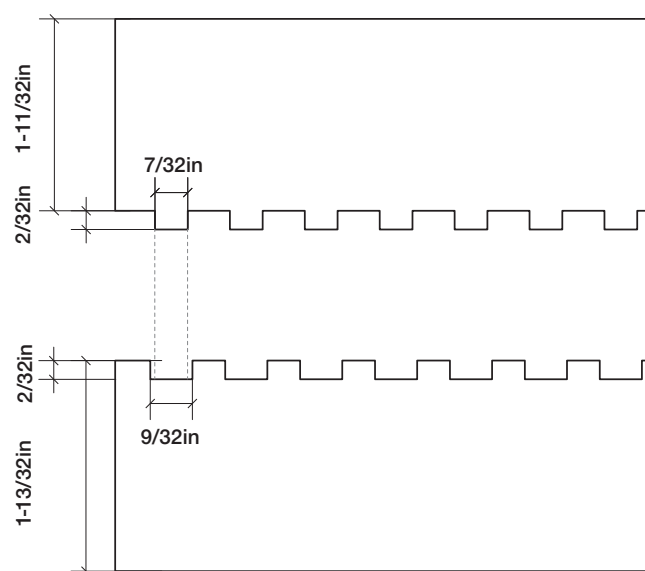

Fig. 18 | Dimensional lumber sizes and milling pattern including tolerance.

respiratory tract related to formaldehyde vapor emissions[58]. When pressed at room temperature, the bonding strength of PVAc adhesives is similar to that of MF resins cured with a hot press at 100 °C[58].

The adhesive was applied to both interface surfaces (each 189 in²) using a scraper tool. One layer was then placed on the other, with the top lumber aligned to the base lumber. The two layers were clamped with parallel clamps at a 6 in spacing along the board, the clamp arm alternating orientation along the beam. The pressure of the parallel clamps was not explicitly controlled. Expressed glue at the edges of the beam was scraped off during the clamping period. An experimental range of between 7.5 in³ and 26 in³ glue was applied in fabricating the beams, and the clamping time varied between 4 and 12 h, as recorded in Table 4. No adhesive was used for the interlocking surface treatments, and all shear between layers was transferred through the contact of the interlocking surfaces.

The metal nail laminating process used 8 d common nails with a shank length L of 2.5 in and a shank diameter D of 0.134 in. Before lamination, the lumber was clamped in place with one parallel clamp at each end of the beam. The nails were driven in using a handheld hammer until the nail head was flush with the wood surface. Nails are driven first at the center of the beam before working towards the ends. The beam was then unclamped, flipped, and reclamped, to allow for nails to be driven from the other side. The flat interface surface treatment followed a tight nail spacing within the allowed limits for fabricating built-up elements according to NDS section 15.3.1 and 15.3.3, with some adjustments as noted in Table 4. Adjacent nails in a row were driven from opposite sides of the beam, in an offset pattern
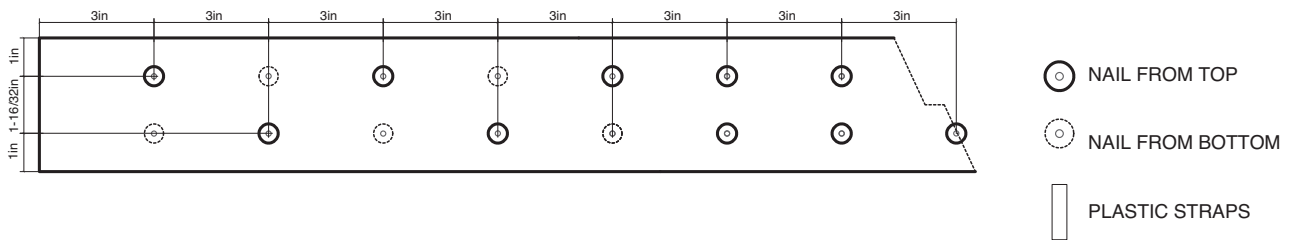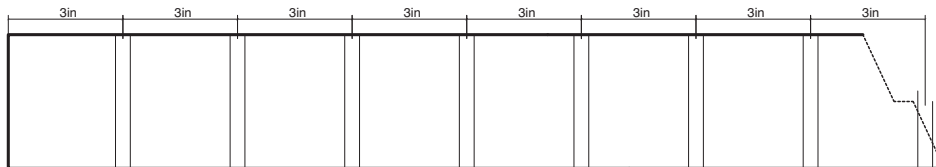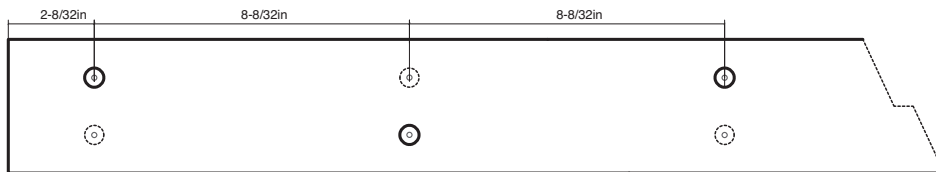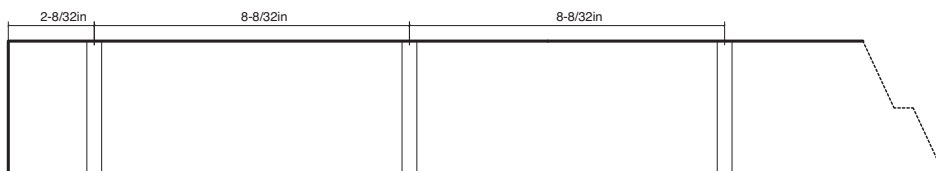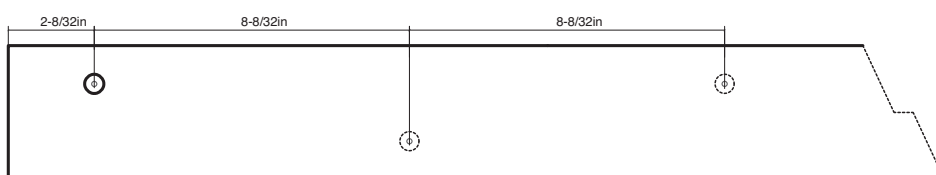
Fig. 19 | Nailing patterns for flat and interlocking interface surfaces. Patterns A and B each have a variation for the use of nails or straps. Pattern C was used for a subset of samples with nails only.

between the two rows. The nails penetrated both layers, and extended through over 80% of the outermost layer, greater than the minimum requirement of 75%. The layers in the beams were less than 1.5 in thick, which does not meet the minimum NDS requirement. The spacing between adjacent nails in a row was 3 in (22.4 D), which is greater than the minimum spacing of 20 D. The spacing between nail rows was 1.5 in (11.2 D), which is greater than the minimum spacing of 10 D and less than the maximum spacing of 20 D. The edge distance was 1 in (7.3 D), which is greater than the
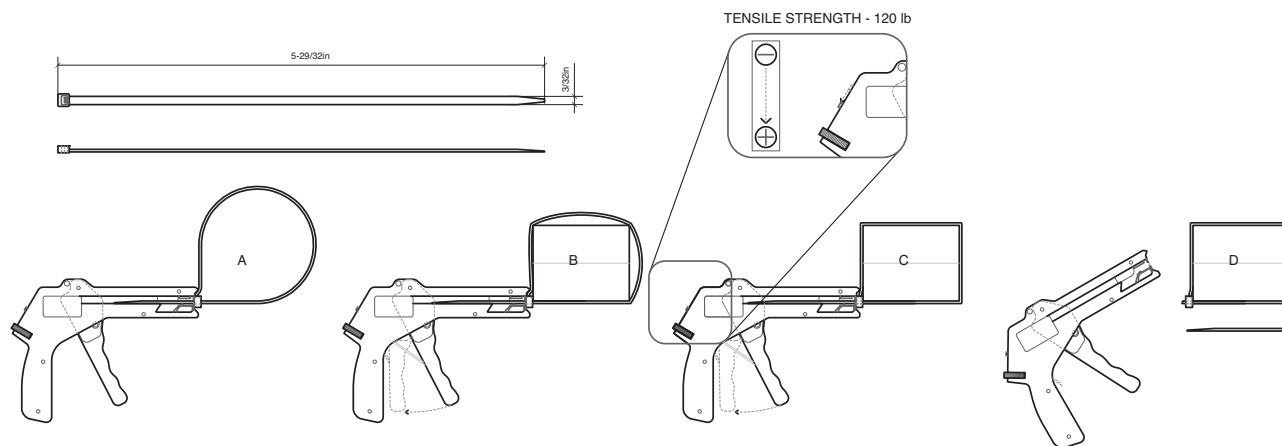
Fig. 20 | Plastic strap installation process. Orientation of strap for installation and step-by-step process for tightening and cutting.
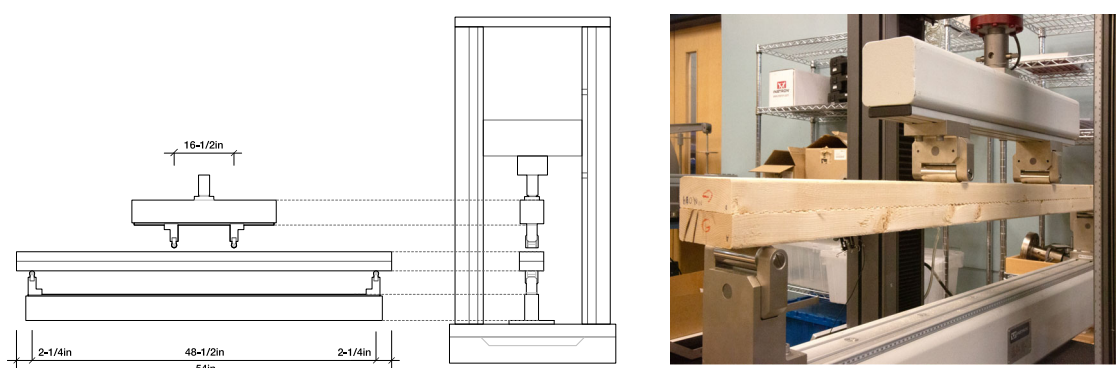
Fig. 21 | Four-point bending laminated beam flexural test setup. Elevation of test distances for support locations and load application points with accompanying photograph of the laboratory setup.

minimum edge distance of 5 D. The end spacing was 3in (22.4 D), which is larger than the maximum end spacing of 18 D. The spacing pattern is shown in Fig. 19.

For the metal nail laminating process with an interlocking interface surface treatment, a wider nail layout also within the allowed limits for fabricating built-up elements according to NDS section 15.3.1 and 15.3.3 was considered, with some adjustments as noted in Table 4. The same nail size and installation method were used for the flat interface surface specimens. The spacing between adjacent nails in a row was 8.25 in, which is equal to the upper spacing limit controlled by 6 times the layer thickness. The nails were installed either in one staggered row with a 1.5 in stagger, or in two rows spaced 1.5 in apart. The edge distance was 1 in (7.3 D), which is greater than the minimum edge distance of 5 D. The end spacing was 2.25 in (16.4 D), which is less than the maximum end spacing of 18D. The spacing pattern is shown in Fig. 19.

The wood nail laminating process followed the same nailing layout as described for the metal nails for the flat interface surface and the interlocking interface surfaces (see Table 4) however, instead of metal nails used a collated nail system made from beech wood produced by BECK was used. The hardwood nails were pneumatically driven into the receiving softwood. The heat generated by driving the wood nail causes the lignin to weld with the surrounding receiving wood. The use of wood nails as opposed to conventional metal nails allows for reduced carbon dioxide emissions associated with the fasteners, avoids nail corrosion, and allows for post-processing of the wood with conventional wood-working tools without risk of damaging the blades. The wood nail system is accompanied by a product performance European Technical Assessment (ETA) document issued by an independent Technical Assessment Body, meaning it can be used in conventional construction.

Compressed beech wood nails of 0.145in diameter and 2in length were used for the lamination process. The difference in length and diameter of the wood nails in comparison to the metal nails was due to the manufacturer's product availability. The short wood nail length means the nail penetrated both layers, but extended through 45% of the outermost layer, less than the minimum requirement of 75%. For the flat interface surface nailing pattern, the spacing between adjacent nails in a row was 3 in (20.7 D), which is greater than the minimum spacing of 20 D. The spacing between nail rows was 1.5 in (10.3 D), which is greater than the minimum spacing of 10 D and less than the maximum spacing of 20 D. The edge distance was 1in (6.9 D), which is less than the minimum edge distance of 5 D. The end spacing was 3in (20.7 D), which is larger than the maximum end spacing of 18 D. For the interlocking interface surface, the edge distance was 1 in (6.9 D), which is greater than the minimum edge distance of 5 D. The end spacing was 2.25 in (15.5 D), which is less than the maximum end spacing of 18 D. The spacing pattern is shown in Fig. 19. The wood nails were installed using a bespoke custom nailer provided by BECK, the F44AC CN15-PS60A LIGNOLOC® FS manufactured by FASCO®. The nailer shoots the nails with a pressure of 7—8 bar (100—115 psi). The pressure was adjusted manually on a wood sample to set the pressure to shoot the nails flush with the surface.

The strap laminating process used nylon plastic wide cable ties to clamp the two laminations together. These cable ties were heavy-duty POWER FIRST 36J168 cable ties are 17.7 in long, 0.3 in wide, and 0.0 8in thick and are rated with a tensile breaking load of 120 lbf. The cable tie installation process involved the use of a C. K Tools 495003 Cable Adjustable Tie Gun with a maximum cable tie capacity of 120 lbf. This tensioning tool does not have specific tension settings but was instead set to the maximum tool capacity using the rotary wheel tension control. The tip of the tie was

pulled through the locking mechanism horizontally, parallel to the interface surface. Once the tensioning tool reached the set tension capacity, it cut the tail of the tie (see Fig. 20). The plastic straps were placed at the same intervals along the beam as the wood and metal nail spacings. For the flat interface surface, the plastic straps were placed at 3 in intervals along the beam, and for the interlocking interface surface, they were placed at 8.5 in intervals.

Nylon cable ties were used as opposed to steel straps to simulate the force application method of an external strap at the comparatively small dimensions of the single-lamination testing samples. The use of nylon cable ties avoided practical impediments in applying and tensioning steel straps at this scale. At full structural dimensions, steel straps would be envisioned to apply external strap forces.

Laminated beam specimen testing protocol

The laminated beam bending tests followed the general testing arrangement outlined in ASTM D198-15—Standard Test Methods of Static Tests of Lumber in Structural Sizes[59], with variations as described. The tests were completed in a four-point bending test (two-point loading configuration in ASTM D198), with the loading heads at the third points between the two support reactions (Fig. 21). The outer span of the beam between supports was 49.5 in. The distance between each loading head and the nearest support was 18.5 in. The beam overhang beyond each support was 2.25 in. The span-depth ratio of the beam was 18. The moisture content of the wood in each testing sample was not recorded at the time of testing. All beam samples were fabricated from wood which had been stored in a conditioned internal environment prior to fabrication and the samples were stored in the conditioned environment (temperature between 20 °C and 22 °C, average humidity of 55%) of the workshop in Rand Hall for a minimum of two weeks post fabrication prior to testing. This allowed the wood to reach a similar controlled moisture content across the samples for a useful comparison between sample test results.

A model 5969 INSTRON UTM was used to complete the tests, with a 2820-044 INSTRON beam bending test apparatus with a maximum capacity of 50 kN and a 50 kN load cell. The load applied to the beam was recorded by the loading head of the UTM. Deflection of the samples during the test was measured at the third points of loading using the measured deflection of the head of the machine, as opposed to a wire or yoke deflectometer. The loading rate was set at 0.1 in/min, with tests taking between 10 min and 20 min to complete.

Laminated beam specimen mechanical property calculation protocol

Mechanical properties for each beam specimen were calculated based on the force and displacement results from the third-point loading configuration, as described in column B of Table X2.1 Flexure Formulas in ASTM D198-15[59]. The MOR was calculated using the maximum bending moment from the maximum load Pmax, the beam span between supports l, and the total beam specimen cross-section width and depth b and d, according to Eq. 4.

$$MOR = \frac{M \cdot c}{I} = \frac{P\max \cdot l}{b \cdot d^2} \qquad (4)$$

Equation 4—*MOR calculation for beam specimen.*

The MOE was calculated for each beam specimen by matching a linear curve to the portion of the force-displacement curve between 20% and 40% of the maximum load, Pmax. The deflection of the beam was recorded through displacement of the loading head on the sample, and not through an additional deflectometer instrumented at the beam center. Therefore, the direct displacement results reflected the displacement at the third-point load application points and not at the beam center. To calculate the beam MOE, a conversion factor was used to relate the deflection at the beam center to the deflection at the loaded third points, calculated using the 'Simple Beam— Two Equal Concentrated Loads Symmetrically Placed' from the Steel Construction Manual[60]. This relationship between deflection at the center of the beam and at the third point is shown in Eq. 5, with the adjusted midpoint

Table 12 | Global warming potential (GWP) impact factor data and sources

Material	Description	GWP data source	GWP			Estimated material source	Distance to workshop
			A1–A3		A4	[Town, State/ Province/ Country]	[miles, type]
			[kgCO2e/m³]	[kgCO2e/1000 kg]	[kgCO2e/short-ton-mile]		
Lumber	North American Softwood lumber	53	39.07			Degelis, Quebec	631, truck
Adhesive	PVAc wood glue	61		2000		Cedar Grove, New Jersey	210, truck
Metal nails	EAF-base wire common nails	62		641		Peru, Illinois	750, truck
Wood nails	Densified beech LignoLoc nails	63		442		Mauerkirchen, Austria	550, truck; 3840, boat; 230, truck
Plastic straps	Nylon 6-6 cable ties	64		10660		Gardner, Massachusetts	300, truck
Truck	Medium and Heavy-Duty Truck	65			0.168		
Boat	Waterborne Craft	65			0.082		
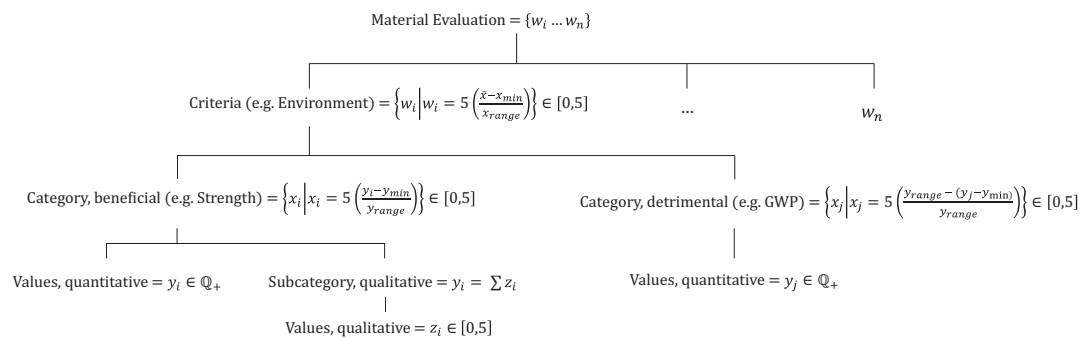
Fig. 22 | Multi-factor evaluation calculation method. Hierarchy tree of the normalization method of beneficial and detrimental values, both quantitative and qualitative.

MOE calculation using the third point deflection shown in Eq. 6.

$$\Delta_{center, a=\frac{l}{3}} : \Delta_{x=\frac{l}{3}} = \frac{23 \cdot P \cdot l^3}{648 \cdot E \cdot I} : \frac{P}{6 \cdot E \cdot I} \left(\frac{l}{3} \right) \left[3 \cdot l \left(\frac{l}{3} \right) - 3 \cdot \left(\frac{l}{3} \right)^2 - \left(\frac{l}{3} \right)^2 \right]$$
$$= 23 : 20 = 1.15 : 1.0$$

(5)

Equation 5—*Relationship between mid-point deflection and third-point deflection for a third-point loaded beam.*

$$MOE = \frac{23 \cdot P \cdot l^3}{108 \cdot b \cdot d^3 \cdot \Delta_{mid}} = \frac{23 \cdot P \cdot l^3}{108 \cdot b \cdot d^3 \cdot (23/20)\Delta_{l/3}}$$

(6)

Equation 6—*MOE calculation for beam specimen based on third-point deflection.*

Non-structural evaluation criteria

In addition to strength and stiffness comparisons between beam lamination methods, the methods can also be compared against non-structural evaluation criteria related to economics, environmental impact, and circularity. For these comparisons, where quantitative data was used, it was determined per one foot length of laminated beam.

Economic data was prepared by recording the individual material purchases and material quantities needed to fabricate each laminated beam, as well as the fabrication processes and fabrication time required to assemble each laminated beam.

The percentage of wood wasted per laminated beam was calculated based on the loss of material due to planing and milling samples before lamination. To ensure that all the laminated beam test specimens had the same overall cross-section, during fabrication of the samples, additional material was removed from the initial feedstock lumber; this material, removed for geometric consistency, was not counted in the comparison. Planning 1/16 in was considered necessary in preparation for applying the adhesive for the flat adhesive laminated beams. Planning 1/16 in to level the sample prior to milling the interlocking pattern specimens was considered necessary to level the material. No planning was considered necessary for the flat non-adhesive lamination methods.

The production time for each sample was prepared as a combination of milling and fabrication. Milling is either the recorded time by the CNC machine or the estimated time apportioned to planing samples. Fabrication is the estimated time apportioned to each process of measuring, fixing locations, nailing, securing ties, spreading glue, or installing clamps. Milling and fabrication are intended to record active manual labor or equipment use and exclude the curing time of any adhesive.

The cost was calculated based on 2024 bulk purchase receipts for lumber and fasteners applied pro rata. Fabrication cost is directly related to the fabrication time and uses a pro-rata cost per hour for a student research assistant of $16/h.

Environmental data was prepared by collecting the quantities of material per foot of each beam lamination method and multiplying each material quantity by the GWP impact factor. The scope of the environmental data was cradle-to-grave, where the site was considered the workshop where the testing sample beams were fabricated. This environmental scope included the GWP impact factor for modules A1–A3 (raw material supply, transport, and manufacture) for each material component, and an estimate of the module A4 transport emissions from the individual supply facilities to the site.

The environmental scope excluded the emissions associated with the energy used in fabrication processes needed to laminate the beam, such as the electricity used in planing and milling, or for the supply of compressed air for the wood nail installation. The GWP impact factors were collected from regional industry average Environmental Product Declarations (EPDs) where possible. Where regional industry average EPDs were not available, impact factors were taken from representative EPDs from individual similar manufacturers or from aggregated databases. GWP impact factors were collected related to the actual materials used in the fabricated testing samples, as opposed to representative beams. This methodology is most notable in the use of the adhesive impact factor (PVAc as opposed to MUF) as further discussed in section 3.3.3. Impact factor source references are indicated with the results in Table 12.

Health impacts were qualitatively assessed based on the presence of VOCs emitted during the use of the product, and on the potential health hazards that would be emitted from the material during manufacture and disposal. The health impacts included here are for the typical adhesive used to laminate glulam commercially—MUF or MF resin—as opposed to the actual adhesive used in this test. This is due to the substitution of a non-toxic PVAc wood glue in the test fabrications to limit the health risk to the research team. The potential for long-term damage from microplastics in the environment is also considered.

Circularity assessments were prepared using a qualitative ranking assignment between 0 and 5 (0 as the worst rating, 5 as the best rating) for each lamination method. The following subcategories were assessed for the *processing* category—*reversibility* of the lamination fastening method, and *machinability* of the fabricated component for future remanufacturing or reuse as is. The following subcategories were considered for the *end-of-life scenario* category—*reuse*, *remanufacturing*, *recycling/composting*, and *incineration/landfill*. *Reversibility* was defined based on whether a fastener could be feasibly removed in the future without damage to the wood; *machinability* was defined as whether conventional woodworking equipment could be used on the complete fabricated component; *reuse* was defined as whether the beam could be used as is in alternative future situations without impediment in a similar function; *remanufacture* was defined as the degree of impediment to future manufacturing, such as permanent changes to wood elements through the cutting of grooves, or the additional processes necessary to remove metal fasteners for reuse in similar or other functions; *recycle/compost* was defined as the suitability of all materials for recycling or decomposition, and whether the element is mono-

material; *Incineration/landfill* was defined related to the level of toxic chemicals that may be released from incineration and uncontrolled dispersion into the environment. This methodology is shown in Table 8.

The overall performance of the lamination methods was evaluated through a simultaneous multi-factor approach where the various category and subcategory results were combined into one value for each of the four evaluation criteria of: structure, economy, environment, and circularity. These combined values were calculated by first converting each subcategory value to a rating between 0 and 5, with the worst performing score defined as zero on the scale, the highest performing score defined as 5, and the intermediate values were scaled linearly between these extremes. The subcategory ratings were then averaged—with an equal weighting between all subcategories—to calculate a combined average value between 0 and 5 for each criterion. The final criteria ratings were then similarly redistributed to calculate a final rating, with the worst performing lamination method assigned a value of zero and the best performing method a value of 5. This methodology is summarized in Fig. 22.

Data availability
Datasets generated during the current study, beyond what is shown in the published article, are available from the corresponding author on reasonable request.

References
1. Asdrubali, F. et al. A review of structural, thermo-physical, acoustical, and environmental properties of wooden materials for building applications. *Build. Environ.* **114**, 307–332 (2017).
2. Norman, J. *Structural Timber Elements: A Pre-scheme Design Guide* (Vol. 1). TRADA. https://bookshop.trada.co.uk/bookshop/view/1F33B2C6-56A0-4552-B8FD-F94954F4FBFD/Structural_timber_elements_a_prescheme_design_guide_2nd_edition (2017).
3. Gauch, H. L., Dunant, C. F., Hawkins, W. & Cabrera Serrenho, A. What really matters in multi-storey building design? A simultaneous sensitivity study of embodied carbon, construction cost, and operational energy. *Appl. Energy* **333**, 120585 (2023).
4. Arlet, J. L. Innovative carpentry and hybrid joints in contemporary wooden architecture. *Arts*. https://doi.org/10.3390/arts10030064 (2021).
5. Safarik, D., Elbrecht, J., & Miranda, W. *State of Tall Timber 2022* (CTBUH Research, 2022).
6. Crocetti, R., Ekholm, K. & Kliger, R. Stress-laminated-timber decks: State of the art and design based on Swedish practice. *Eur. J. Wood Wood Products* **74**, 453–461 (2016).
7. Alderman, D. *U.S. Forest Products Annual Market Review and Prospects, 2015–2021* (USDA, 2022).
8. Ramage, M. et al. *The Wood From the Trees: The Use of Timber in Construction*. https://doi.org/10.1016/j.rser.2016.09.107 (2017).
9. Ashby, M. F. Chapter 4—material property charts. In *Materials Selection in Mechanical Design* 4th edn (ed. Ashby, M. F.) 57–96 (Butterworth-Heinemann, 2011); https://doi.org/10.1016/B978-1-85617-663-7.00004-7
10. NYCEDC. *Clean and Circular: Design and Construction Guidelines* (NYCEDC, 2024).
11. Heisel, F., Hebel, D. E., & Webster, K. *Building Better—Less—Different: Circular Construction and Circular Economy* (Birkhäuser; 2022); https://birkhauser.com/books/9783035626353
12. Potting, J., Hekkert, M., Worrell, E., & Hanemaaijer, A. *Circular Economy: Measuring Innovation in The Product Chain* (PBL Netherlands Assessment Agency, 2017).
13. AITC. *AITC TN-26: Design Values for Structural Glued Laminated Timber in Existing Structures* (AITC, 2007); https://plib.org/wp-content/uploads/2020/05/AITC-TN-26-2007.pdf
14. Yahmi, A. et al. Mind-mapping assessment of reuse potential of glulam: an experimental study. *Buildings*. https://doi.org/10.3390/buildings13122929 (2023).
15. ICC. *Chapter 23 Wood—2021 International Building Code (IBC)* (ICC, 2021); https://codes.iccsafe.org/content/IBC2021P2/chapter-23-wood
16. ANSI. *ANSI A190.1-2022 Product Standard for Structural Glued Laminated Timber* (ANSI, 2022)
17. British Standards Institution. *BS EN 14080:2013 Timber structures—Glued Laminated Timber and Glued Solid Timber—Requirements* (The British Standards Institution, 2013)
18. Bergsagel, D. & Heisel, F. Structural design using reclaimed wood—a case study and proposed design procedure. *J. Clean. Prod.* **420**, 138316 (2023).
19. Bergsagel, D., Isaac, P., & Koeck, A. *Feasibility Study Exploring Turning Reclaimed Timber into Structural Glulam* (CIRCUIT, 2022).
20. Bergman, R. D., Falk, R. H., Gu, H., Napier, T. R., & Meil, J. *Life-Cycle Energy and GHG Emissions for New and Recovered Softwood Framing Lumber and Hardwood Flooring Considering End-of-Life Scenarios* (No. FPL-RP-672; p. FPL-RP-672) (U.S. Department of Agriculture, Forest Service, Forest Products Laboratory, 2023); https://doi.org/10.2737/FPL-RP-672
21. Peng, L., Searchinger, T. D., Zionts, J. & Waite, R. The carbon costs of global wood harvests. *Nature* **620**, 110–115 (2023).
22. EPA. *AP 42, Compilation of Air Pollutant Emissions Factors from Stationary Sources*, *5th Edition, Volume I Chapter 10.9 Engineered Wood Products*. https://www.epa.gov/sites/default/files/2020-10/documents/c10s09.pdf (2002).
23. Hussin, M. H. et al. Latest advancements in high-performance bio-based wood adhesives: a critical review. *J. Mater. Res. Technol.* **21**, 3909–3946 (2022).
24. International Living Future Institute. *Living Building Challenge 4.1—Program Manual* (LIVING FUTURE, 2024).
25. Puettmann, M. E., & Wilson, J. B. Gate-to-gate life-cycle inventory of glued-laminated timbers production. *Wood Fiber Sci.* **37**, 99–113 (2005).
26. Crocetti, R. *Large-Span Timber Structures* (The World Congress on Civil, Structural, and Environmental Engineering, 2016); https://doi.org/10.11159/icsenm16.124
27. Holt, R., Luthi, T., & Dickof, C. *Nail-Laminated Timber—U.S. Design & Construction Guide v1.0.* (Binational Softwood Lumber Council, 2017)
28. Guan, Z. et al. *Development Of Adhesive Free Engineered Wood Products—Towards Adhesive Free Timber Buildings* (WCTE, 2018).
29. Dourado, N., Pereira, F. A. M., Lousada, J. L. & de Moura, M. F. S. F. Experimental and numerical analyses of wood boards joining using wood-pin connectors. *Constr. Build. Mater.* **222**, 556–565 (2019).
30. O'Loinsigh, C. et al. Experimental study of timber-to-timber composite beam using welded-through wood dowels. *Constr. Build. Mater.* **36**, 245–250 (2012).
31. Widmann, R. Screw-laminated timber deck plates. *IABSE Conference, Lahti 2001: Innovative Wooden Structures and Bridges*, 223–228 (IABSE, 2001); https://doi.org/10.2749/222137801796348548
32. AWC. *2018 National Design Specification for Wood Construction* (American Wood Council, 2017).
33. Sotayo, A. et al. Review of state of the art of dowel laminated timber members and densified wood materials as sustainable engineered wood products for construction and building applications. *Dev. Built Environ.* **1**, 100004 (2020).
34. Supe, P. & Iejavs, J. Bending properties of mechanically jointed solid timber beams. *Drewno* **60**, 151–159 (2017).
35. Rombach Bauholz und Abbund GmbH. *NUR-HOLZ: The Solid Timber Construction Method from the German Black Forest*. https://www.nur-holz.com/fileadmin/user_upload/aktuelles/Download/Brochure_NUR_HOLZ_2015_English_zum_versenden.pdf (2015).

36. Arup. (n.d.). *People's Pavilion* (Retrieved 10 Jan 2025); https://www.arup.com/projects/peoples-pavilion/

37. Kumar, C. & Leggate, W. An overview of bio-adhesives for engineered wood products. *Int. J. Adhes.* **118**, 103187 (2022).

38. Rammer, D. R., de Melo Moura, J., & Ross, R. J. *Structural Performance of the Second Oldest Glued-Laminated Structure in the United States* 1233–1243 (2014); https://doi.org/10.1061/9780784413357.111

39. Stalnaker, J. J., & Harris, E. C. Glued Laminated Members. In S*tructural Design in Wood* (eds. Stalnaker, J. J. & Harris, E. C.) 157–198 (Springer, 1997); https://doi.org/10.1007/978-1-4615-4082-3_8

40. Nakos, P., Achelonoudis, C., Papadopoulou, E., & Karagiannidis, E. *Environmentally-Friendly Adhesives For Wood Products Used In Construction Applications. WTCE 2016. World Conference on Timber Engineering* (WTCE, Vienna, 2016).

41. Mary, A., Blanchet, P., Pepin, S., Chamberland, J., & Landry, V. Upcycling of protein concentrates from industrial byproducts into polyurethane wood adhesives. *BioResources* **19**, 1 (2024).

42. Heisel, F., McGranahan, J., Lucas, A., Cohen, D. & Stone, G. Carbon, economics, and labor: a case study of deconstruction's relative costs and benefits compared to demolition. *J. Phys. Conf. Ser.* **2600**, 192003 (2023).

43. Heisel, F., Minner, J., Augustine-Marceil, W., Cohen, D., & Worth, G. *Constructing a Circular Economy in New York State: Deconstruction and Building Material Reuse* (Cornell Circular Construction Lab, Cornell Just Places Lab, and CR0WD, 2024); https://labs.aap.cornell.edu/ccl/whitepaper

44. Arbelaez, R., Schimleck, L. & Sinha, A. Salvaged lumber for structural mass timber panels: manufacturing and testing. *Wood Fiber Sci.* **52**, 178–190 (2020).

45. Dong, W., Rose, C. M. & Stegemann, J. A. Cross-laminated secondary timber: validation of non-destructive assessment of structural properties by full-scale bending tests. *Eng. Struct.* **298**, 117029 (2024).

46. Llana, D. F., Iniguez-Gonzalez, G., de Arana-Fernandez, M., Ui Chulain, C., & Harte, A. M. Recovered wood as raw material for structural timber products. Characteristics, situation and study cases: Ireland and Spain. *Renewable Resources for a Sustainable and Healthy Future—Proceedings of the 2020 Society of Wood Science and Technology International Convention* 1–833 (SWST, 2020); https://doi.org/10.22382/proc-2020-02

47. Rose, C. M. et al. *Cross-Laminated Secondary Timber: Experimental Testing and Modelling the Effect of Defects and Reduced Feedstock Properties* (MDPI, 2018).

48. Cousins, S. *Structural Timber Prototype Uses 100% Waste from Demolition* (RIBA, 2024).; https://www.ribaj.com/products/structural-timber-prototype-uses-waste-from-demolition-ucl-circular-economy

49. *UK CLT* (n.d.) (Retrieved 21 January 2025); https://ukclt.com/

50. Gassman, J. R. The Kendeda building for innovative sustainable design: acting at the intersection of carbon, health and equity. In *Building Better—Less—Different: Circular Construction and Circular Economy* (ed. Heisel, F. & Hebel, D. E.) 104–107) (Birkhäuser, 2022).

51. Asa, P. et al. Embraced wood: circular construction method for composite long-span beams from unprocessed reclaimed timber, fibers and clay. *Constr. Build. Mater.* **416**, 135096 (2024).

52. Browne, X., Larsen, O. P., Friis, N. C. & Kühn, M. S. Material value(s): motivating the architectural application of waste wood. *Archit. Struct. Constr.* **2**, 575–584 (2022).

53. Athena Sustainable Materials Institute. *A Cradle-to-Gate Life Cycle Assessment of Eastern Canadian Surfaced Dry Softwood Lumber* (2018).

54. ASTM. *ASTM D 143—14: Standard Test Methods for Small Clear Specimens of Timber* (ASTM International, 2014); https://doi.org/10.1520/D0143-14

55. ASTM. *ASTM D 905—98: Standard Test Method for Strength Properties of Adhesive Bonds in Shear by Compression Loading* (ASTM International, 1998).

56. British Standards Institution. *Eurocode 5: Design of Timber Structures—Part 1-1: General—Common Rules and Rules for Buildings, Annex B (Informative): Mechanically Jointed Beams* (The British Standards Institution, 2014).

57. Jeong, G. Y., Pham, V. S. & Tran, D. K. Development of predicting equations for slip modulus and shear capacity of CLT–concrete composite with screw connections. *J. Build. Eng.* **71**, 106468 (2023).

58. Kim, S. & Kim, H.-J. Effect of addition of polyvinyl acetate to melamine-formaldehyde resin on the adhesion and formaldehyde emission in engineered flooring. *Int. J. Adhes. Adhesives* **25**, 456–461 (2005).

59. ASTM. *ASTM D 198—15: Standard Test Methods of Static Tests of Lumber in Structural Sizes* (ASTM International, 2015); https://doi.org/10.1520/D0198-15

60. AISC. *Steel Construction Manual* 16th edn (American Institute of Steel Construction, 2023).

61. Dana Lim A/S. *Environmental Product Declaration EPD-DBC-20220147-IBF1-EN, Dispersion-Based Products, Group 2: Wood Glue D2 Outdoor 430, Laminate Floor Glue 433, Wood Glue D4 Outdoor 440* https://dl2phipa8wx75.cloudfront.net/danalim/downloads/1670589241-q0q-EPD.pdf (2022).

62. ArcelorMittal Europe. *Environmental Product Declaration S-P-11875, Nails EAF-Base* https://api.environdec.com/api/v1/EPDLibrary/Files/060e7a69-aba4-41af-1a36-08dc25c78130/Data (2024).

63. vom Berg, C., & Carus, M. *Life Cycle Assessment (LCA) of the LignoLoc wooden nail—Summary of the full LCA Report* (Nova Institute, 2019).

64. OEKOBAU.DAT. *Nylon Gusstel (PA 6.6)* https://www.oekobaudat.de/OEKOBAU.DAT/datasetdetail/process.xhtml?lang=de&uuid=7511c948-c441-42fb-9ff1-cfdc54e58d7e (2018).

65. Environmental Protection Agency. *Emission Factors for Greenhouse Gas Inventories* https://www.epa.gov/system/files/documents/2024-02/ghg-emission-factors-hub-2024.pdf (2024).

Acknowledgements

Author contributions

D.B.: conception, first draft, project management, calculations, data post-processing, and review and editing. F.H.: conception, project management, funding, circularity analysis, diagrams, draft, and review and editing. J.O.: testing rig manufacture, specimen manufacture, testing, and diagrams. M.R.: testing rig manufacture, specimen manufacture, and testing.

Competing interests

The authors declare no competing interests.

Additional information

Correspondence and requests for materials should be addressed to Felix Heisel.